



RESEARCH ARTICLE

Proteomic comparison between non-purified cerebrospinal fluid and cerebrospinal fluid-derived extracellular vesicles from patients with Alzheimer's, Parkinson's and Lewy body dementia

Yael Hirschberg^{1,2}  | Natalia Valle-Tamayo^{3,4} | Oriol Dols-Icardo^{3,4} |
 Sebastiaan Engelborghs^{5,6} | Bart Buelens⁷ | Roosmarijn E. Vandenbroucke^{8,9}  |
 Yannick Vermeiren^{10,11} | Kurt Boonen^{1,2} | Inge Mertens^{1,2}

¹Health Unit, Flemish Institute for Technological Research (VITO), Mol, Belgium

²Centre for Proteomics (CfP), University of Antwerp, Antwerp, Belgium

³Department of Neurology, Sant Pau Memory Unit, Sant Pau Biomedical Research Institute, Hospital de la Santa Creu i Sant Pau, Universitat Autònoma de Barcelona, Barcelona, Spain

⁴Network Center for Biomedical Research in Neurodegenerative Diseases (CIBERNED), Madrid, Spain

⁵Department of Neurology and Bru-BRAIN, Universitair Ziekenhuis Brussel and NEUR Research Group, Center for Neurosciences (C4N), Vrije Universiteit Brussel (VUB), Brussels, Belgium

⁶Department of Biomedical Sciences, University of Antwerp, Antwerp, Belgium

⁷Data Science Hub, Flemish Institute for Technological Research (VITO), Mol, Belgium

⁸VIB Center for Inflammation Research, VIB, Ghent, Belgium

⁹Department of Biomedical Molecular Biology, Ghent University, Ghent, Belgium

¹⁰Faculty of Medicine & Health Sciences, Translational Neurosciences, University of Antwerp, Antwerp, Belgium

¹¹Division of Human Nutrition and Health, Chair Group of Nutritional Biology, Wageningen University & Research (WUR), Wageningen, The Netherlands

Correspondence

Yael Hirschberg and Inge Mertens, Health Unit, Flemish Institute for Technological Research (VITO), Mol, Belgium.
 Email: yael.hirschberg@vito.be and inge.mertens@vito.be

Funding information

Alzheimer's Association, Grant/Award Number: AARF-22-924456; Carlos III Health Institute, Grant/Award Number: FI22/00077; Flemish Institute for Technological Research

Abstract

Dementia is a leading cause of death worldwide, with increasing prevalence as global life expectancy increases. The most common neurodegenerative disorders are Alzheimer's disease (AD), dementia with Lewy bodies (DLB) and Parkinson's disease dementia (PDD). With this study, we took an in-depth look at the proteome of the (non-purified) cerebrospinal fluid (CSF) and the CSF-derived extracellular vesicles (EVs) of AD, PD, PD-MCI (Parkinson's disease with mild cognitive impairment), PDD and DLB patients analysed by label-free mass spectrometry. This has led to the discovery of differentially expressed proteins that may be helpful for differential diagnosis. We observed a greater number of differentially expressed proteins in CSF-derived EV samples ($N = 276$) compared to non-purified CSF ($N = 169$), with minimal overlap between both datasets. This finding suggests that CSF-derived EV samples may be more suitable for the discovery phase of a biomarker study, due to the removal of more abundant proteins, resulting in a narrower dynamic range. As disease-specific markers, we selected a total of 39 biomarker candidates identified in non-purified CSF, and 37 biomarker candidates across the different diseases under investigation in the CSF-derived EV data. After further exploration and

This is an open access article under the terms of the [Creative Commons Attribution-NonCommercial-NoDerivs License](https://creativecommons.org/licenses/by-nc-nd/4.0/), which permits use and distribution in any medium, provided the original work is properly cited, the use is non-commercial and no modifications or adaptations are made.

© 2023 The Authors. *Journal of Extracellular Vesicles* published by Wiley Periodicals LLC on behalf of International Society for Extracellular Vesicles.

validation of these proteins, they can be used to further differentiate between the included dementias and may offer new avenues for research into more disease-specific pharmacological therapeutics.

KEYWORDS

biomarkers, cerebrospinal fluid, dementia, extracellular vesicles, mass spectrometry, proteomics

1 | INTRODUCTION

Dementia is a leading cause of death worldwide, with increasing prevalence as global life expectancy increases (Prince et al., 2016). The most common neurodegenerative disorder causing dementia is Alzheimer's disease (AD), followed by dementia with Lewy bodies (DLB) and Parkinson's disease dementia (PDD) (Vann Jones & O'Brien, 2014). Whereas AD is primarily characterised by cognitive dysfunction and neuropsychiatric symptoms, DLB and PDD are additionally featured by a movement disorder. Dementia affects about 25%–50% of patients with Parkinson's disease (PD) (Williams-Gray et al., 2013), which is categorised under the umbrella term of PDD. In clinical practice, DLB is frequently misdiagnosed as AD because of the similar clinical and pathological features. Indeed, ¾ of the DLB patients have AD co-pathology in the brain, leading to an AD-like cerebrospinal fluid (CSF) AD core biomarker profile (Slaets et al., 2013). To differentiate between PDD and DLB, there is a current debate about whether PDD and DLB are one or different pathologies (Jellinger & Korczyn, 2018), but, generally, the arbitrary one-year rule is applied (Mckeith et al., 2017). This rule is solely based on the onset of the cognitive impairment and states that the patient is diagnosed with PDD if dementia develops 1 year or more after the motor symptoms. In case these two symptoms develop within the same year, or, if the cognitive impairment is observed before the motor symptoms, DLB should be diagnosed (Yamada et al., 2020). This rule is hard to apply in clinical practice, and even more so at the end stage of both diseases due to almost identical characteristics. Studies attempting to differentiate between both diseases have observed that the motor symptoms, typical for PD, such as tremor, rigidity and akinesia, tend to be more severe in PDD than in DLB (Fritz et al., 2016). However, parkinsonism of increasing severity is observed in DLB patients over time, with a prevalence ranging from 60% to 92% (Ferman et al., 2011). It is worth noting that 18%–25% of DLB patients do not develop severe parkinsonian symptoms (Outeiro et al., 2019). Also cognitive differences have been discussed previously (Smirnov et al., 2020). DLB is associated with more severe cognitive deficits, more frequent hallucinations and a more rapid disease progression (Devanand et al., 2022). It is important to note that medications are typically developed for a single pathology and may have adverse effects when administered to populations with a different (co-) pathology. Furthermore, these therapies are often not tested properly in other populations, thus their effects cannot always be accurately predicted. For instance, the newly FDA-approved AD disease-modifying drugs, such as lecanemab, were developed specifically for AD and as such will probably not show any positive effects on DLB patients (Van Dyck et al., 2023). However, a differential diagnosis between, for instance, AD and DLB is still challenging because of overlapping PET and CSF biomarkers but required for appropriate medication. In addition, previous research has reported that up to 89% of PDD patients experience at least one neuropsychiatric symptom (Aarsland et al., 2007). But unlike in AD, the use of atypical antipsychotics in PDD and DLB patients poses a clinical challenge due to the blockage of dopamine (D2) receptors by these medications, which can exacerbate motor symptoms in PD (Ballard & Howard, 2006). Hypersensitivity to antipsychotics, also atypical ones acting on other receptors, is even a diagnostic criterium for DLB (Mckeith et al., 2017) and is thus contra-indicated. In line with previously mentioned shortcomings, it is, therefore, most optimal to provide a disease-specific clinical diagnosis already in the prodromal phase. Although most biomarker research focusses on distinguishing disease from healthy, some work has also been done on improving differential diagnosis among neurodegenerative disorders, as reviewed by Bousiges and Blanc (2022).

It has been a matter of debate as to how the pathogenic proteins of amyloid beta ($A\beta$) deposits, tau neurofibrillary tangles and α -synuclein Lewy bodies spread throughout the brain. Tau and α -synuclein have been shown to spread in a predictable, characteristic pattern as the result of cell-to-cell transmission in a prion-like manner. This way, they show the ability to self-propagate via templated misfolding and intercellular dissemination (Uemura et al., 2020). Several studies have reported the possible role of extracellular vesicles (EVs) in this cell-to-cell transmission. Recently, the pathogenic species of α -synuclein, which could initiate oligomerisation of soluble α -synuclein in target cells and confer disease pathology, was also detected in CSF-derived EVs (Stuendl et al., 2016). Previous studies also reported that certain forms of tau are present in EVs (Dujardin et al., 2014; Fiandaca et al., 2015; Kanmert et al., 2015; Wang et al., 2017), and some investigators have suggested that tau contained in EVs may facilitate aggregation of tau in recipient cells (Wang et al., 2017; Winston et al., 2016). Next, $A\beta$ was already identified in CSF-derived EVs from an AD mouse model (Yuyama et al., 2014) and in blood neuronal-derived extracellular vesicles (Li et al., 2022). These data support the hypothesis that neuronal EVs play an important role in disease progression and that these can be found in CSF, serving as an excellent source of biomarkers, which is what will be explored in this study. Here, we compare the non-purified CSF and CSF-derived EV proteome of AD, PD, PD-MCI, PDD and DLB patients analysed by label-free mass spectrometry. To our knowledge, this is the first study to compare both sample types, and to compare the CSF-derived EV proteome between these

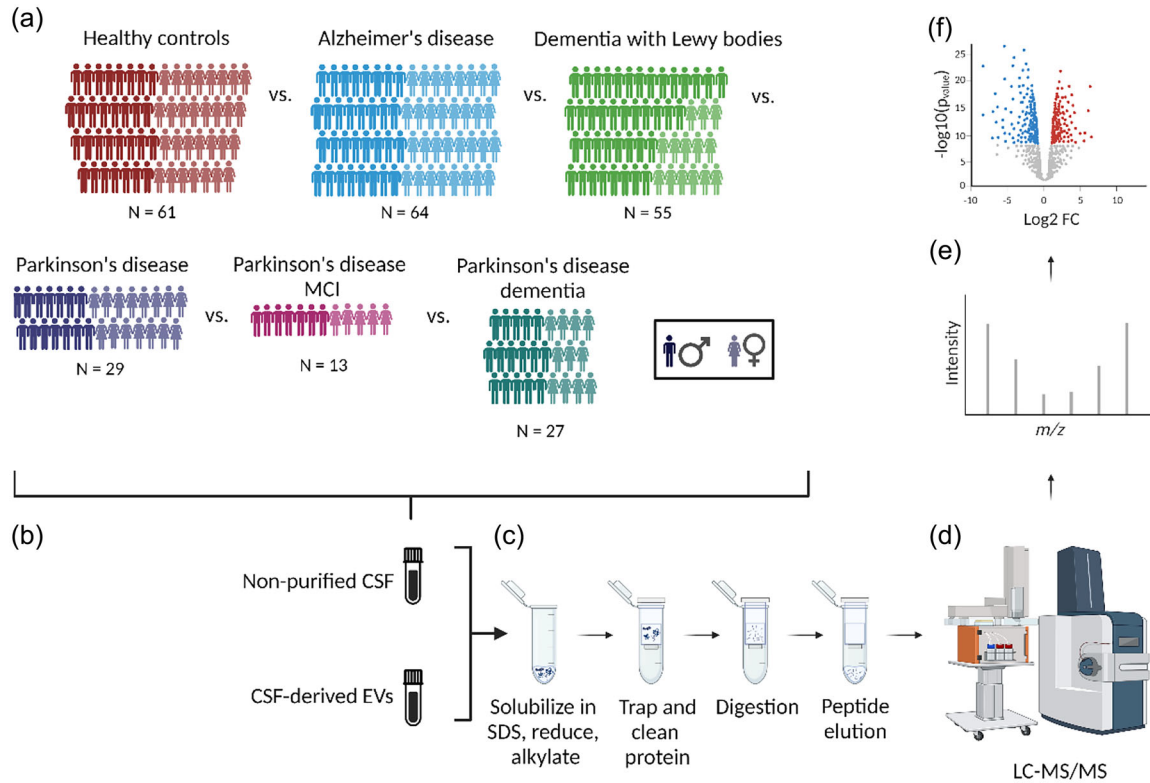


FIGURE 1 Overview of the study. (a) The sample cohort detailed in sections ‘Study population’ and ‘CSF collection and metadata’. (b) The acquisition of two sample types, as outlined in section ‘Isolation of extracellular vesicles’. (c) The sample preparation steps for LC-MS/MS, as described in section ‘Protein extraction and S-trap digestion’, (d) The instruments used according to section ‘Liquid chromatography tandem mass spectrometry (LC-MS/MS) analysis’, (e) LC-MS/MS output results being peptide intensity on the Y-axis and m/z on the X-axis, as used in section ‘Peptide identification’. (f) A volcano plot to present the differential data analysis as performed in R, see section ‘Differential analysis’. CSF, cerebrospinal fluid; EVs, extracellular vesicles; FC, fold change; LC-MS/MS, liquid chromatography tandem mass spectrometry; MCI, mild cognitive impairment; m/z , mass to charge ratio; N , number of samples. Created with BioRender.com.

different dementia subtypes. Prior, two studies have been performed comparing CSF-derived EV proteome between healthy controls and AD patients (Chatterjee et al., 2023; Muraoka et al., 2020). Muraoka et al. (2020) found three dysregulated proteins (being HSPA1A, NPEPPS and PTGFRN), while Chatterjee et al. (2023) found 26 upregulated proteins in AD and 88 downregulated proteins. The goal of our study is to identify novel biomarker candidates that have high potential for differential diagnosis, or that potentially provide targets for novel or repurposed pharmacotherapeutics.

2 | METHODS

2.1 | Graphic study overview

2.1.1 | Study population

The study included CSF samples of 249 subjects, including patients with AD, PD, PD-MCI, PDD, DLB and cognitively healthy controls (HC) (Figure 1a, Table 1). Samples were retrospectively selected from the NeuroBiobank of the Institute Born-Bunge (NBB-IBB, federal agency for medicines and health products registration number 190113; Antwerp, Belgium). All participants were originally recruited from the Memory Clinic of the Hospital Network Antwerp (ZNA-Middelheim and ZNA-Hoge Beuken, Antwerp, Belgium) between 1992 and 2018, as part of their diagnostic clinical work-up.

The clinical diagnosis of probable AD was based on the NINCDS/ADRDA criteria of Mckhann et al. (1984, 2011) whereas probable DLB was diagnosed according to the consensus guidelines of McKeith et al. (2005, 1996). In addition, AD patients had to fulfil the international work group criteria-2 (IWG-2) during clinical diagnosis (Dubois et al., 2014). Twenty-five patients within this cohort also consented to a *post-mortem* neuropathological immunohistochemical investigation, that confirmed their clinical diagnoses (i.e., resulting into definite AD or DLB) (Table 1: Definite diagnosis) (Vermeiren et al., 2015). Subjects were diagnosed with PD according to protocol and criteria as described previously (Engelborghs et al., 2003). PD patients were classified as PD, PD-MCI or PDD based on the conclusion reports of extensive neuropsychological assessments from no more than three months

TABLE 1 Demographics and sample information.

	AD	PD	PD-MCI	PDD	DLB	HC
Subjects—N	64	29	13	27	55	61
Age—years						
Median	76	70	80	78	75	65
Minimum—maximum	56–89	36–83	67–85	66–88	61–90	54–88
Storage time						
0–5 years	21 (33%)	0 (0%)	0 (0%)	2 (7%)	3 (5%)	11 (18%)
5–10 years	39 (61%)	1 (3%)	0 (0%)	1 (4%)	3 (5%)	24 (39%)
10–15 years	4 (6%)	3 (11%)	1 (8%)	3 (11%)	14 (26%)	0 (0%)
15–20 years	0 (0%)	10 (34%)	2 (15%)	18 (67%)	23 (42%)	26 (43%)
>20 years	0 (0%)	15 (52%)	10 (77%)	3 (11%)	12 (22%)	0 (0%)
Sex—N						
Male	32 (50%)	14 (48%)	8 (62%)	16 (59%)	41 (75%)	31 (51%)
Female	32 (50%)	15 (52%)	5 (38%)	11 (41%)	14 (25%)	30 (49%)
C-fraction—N						
C1	54 (84%)	11 (38%)	2 (15%)	16 (59%)	33 (60%)	11 (18%)
C2	1 (2%)	0 (0%)	0 (0%)	0 (0%)	0 (0%)	0 (0%)
C3	3 (5%)	0 (0%)	0 (0%)	0 (0%)	0 (0%)	25 (41%)
C4	6 (9%)	0 (0%)	1 (8%)	2 (7%)	5 (9%)	3 (5%)
C5	0 (0%)	0 (0%)	0 (0%)	0 (0%)	2 (4%)	0 (0%)
Unknown	0 (0%)	18 (62%)	10 (77%)	9 (33%)	15 (27%)	22 (36%)
Previous F/T cycli—N						
0	48 (75%)	24 (83%)	7 (54%)	21 (78%)	35 (64%)	56 (92%)
1	12 (19%)	4 (14%)	5 (38%)	6 (22%)	15 (27%)	5 (8%)
2	4 (6%)	0 (0%)	1 (8%)	0 (0%)	2 (4%)	0 (0%)
3	0 (0%)	1 (3%)	0 (0%)	0 (0%)	3 (5%)	0 (0%)
Definite diagnosis—N	14	0	0	2	9	NTA
MMSE score known—N	48	0	0	0	0	8

Abbreviations: AD, Alzheimer's disease; C-fraction, the collection of cerebrospinal fluid in 1 out of 5 consecutive fractions following lumbar puncture (C1 being the first fraction collected and C5 the last); DLB, dementia with Lewy bodies; F/T, freeze/thaw; HC, healthy controls; MMSE, Mini-Mental State Examination; N, number of samples; NTA, not applicable; PD, Parkinson's disease; PDD, Parkinson's disease dementia.; PD-MCI, Parkinson's disease with mild cognitive impairment.

before or after date of sampling. All patients also fulfilled the Diagnostic and Statistical Manual of Mental Disorders-IV- text revision (DMS-IV-TR) criteria (American Psychiatric Association, 2010).

HCs were sampled between 2002 and 2017 and had no neurological nor psychiatric antecedents or an organic disease involving the central nervous system. All HCs were hospitalised during the time of their lumbar puncture and mainly consisted of (i) subjects complaining of low back pain requiring a selective lumbar radiculography; (ii) patients with disorders of the peripheral nervous system (peripheral facial nerve palsy) and (iii) patients with subjective complaints in whom disorders of the central and peripheral nervous system were ruled out by means of an extensive clinical work-up (Engelborghs et al., 2008). HCs were younger at the time of CSF collection in comparison to AD (p -value = 0.0124), DLB (p -value = 0.0041), PD-MCI (p -value = 0.0109) and PDD (p -value = 0.0003) (Table 1). Our study was conducted in compliance with the Helsinki Declaration, and Ethics Approval for human sample collection of CSF and *post-mortem* brain obduction was granted by the Medical Ethical Committee of the Middelheim General Hospital (Antwerp, Belgium; approval numbers 2805 and 2806).

2.2 | CSF collection and metadata

CSF sampling was performed as described previously (Somers et al., 2016). In short, a lumbar puncture was performed at the L3/L4 or L4/L5 interspace between 08.00 and 10.00 a.m., after overnight fasting and having abstained from smoking for at least 12 h. Morning medication was administered after the lumbar puncture. A total of 16.5 mL was collected stepwise in five fractions (polypropylene vials; Nalgene; VWR, Leuven, Belgium) (referred to as C-fractions): fraction C1 (4.5 mL), C2 (1.5 mL),

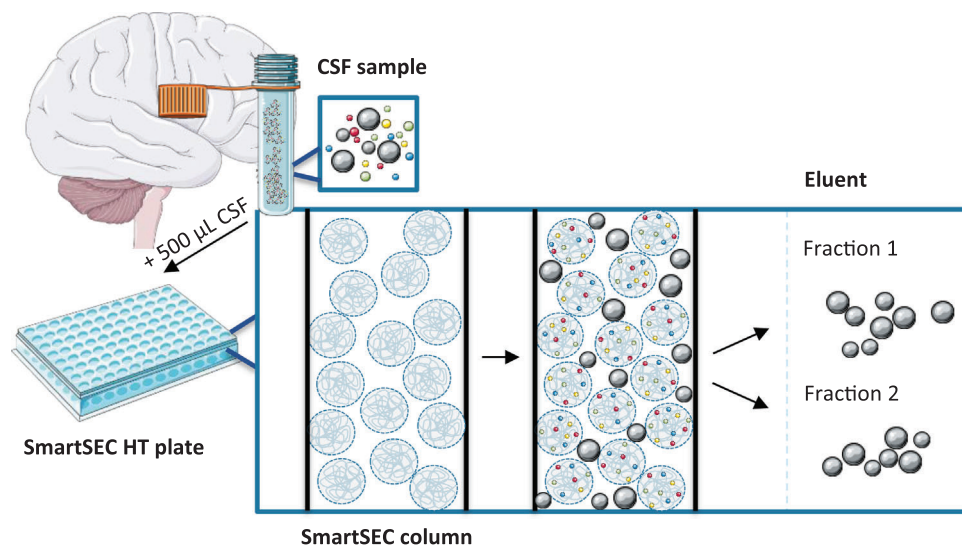


FIGURE 2 Illustration of the SmartSEC EV isolation technique, performed on aliquots number one. Particles that can pass the size exclusion columns are collected in the eluent, while small proteins (up to 400 kDa) enter the bead core and, because of affinity interaction modes, stay trapped. Figure adapted from System Biosciences, with Figures from smart.servier.com (licensed under CC BY 3.0). CSF, cerebrospinal fluid; HT, high throughput; SEC, size exclusion chromatography.

C3 (1.5 mL), C4 (4.5 mL) and C5 (4.5 mL). Fractions C1 to C4 were immediately frozen in liquid nitrogen. Fraction C5 was centrifugated (Centrifuge 5702, rotor A-4-38; Eppendorf, Hamburg, Germany) on 3000 rpm for 10 min, after which the supernatant was divided over three vials, which were then frozen in liquid nitrogen as well.

For this study, the selection of fraction and preceding freeze/thaw (F/T) cycle was based upon availability (Table 1). Haemolysis was checked visually (exclusion criterium: light pinkish) to avoid potential oxidation and contamination effects. Six samples of the cohort were observed to be slightly haemolytic. For some AD and HC CSF samples, analyses of $A\beta_{1-42}$, total tau (T-Tau), and hyperphosphorylated tau (pTau181) were previously performed by means of ELISA, as part of a routine diagnostic procedure. The detailed CSF analyses protocol has already been published before (Somers et al., 2016).

In general, of each frozen CSF sample, two aliquots of 500 μ L (aliquot number one and aliquot number two, Figure 1b) were taken and re-frozen at -80°C , inducing an additional F/T cycle. For two exceptions, not sufficient volume of CSF was available for two aliquots and only one aliquot (i.e., aliquot number one) was stored. One other sample had too little volume available for EV isolation, so was only used as aliquot number two. Aliquots number one were used for EV isolation ($N = 249$), while aliquots number two ($N = 248$) were not enriched prior to analyses and kept stored at -80°C until LC-MS/MS (liquid chromatography tandem mass spectrometry) sample preparation.

2.3 | Isolation of extracellular vesicles

Of each frozen CSF sample, two aliquots were available. Aliquots number one (500 μ L of CSF, $N = 249$) were thawed on ice and centrifuged 10 min at $2500 \times g$ to remove cell debris prior to EV isolation using the SmartSEC HT kit (System Biosciences) according to manufacturer's instructions (Figure 2). After preparing the SmartSEC filter plate, samples were loaded into the wells. Following an incubation step of 30 min at room temperature, the first SEC fraction was collected by centrifuging the plate for 2 min at $500 \times g$. All centrifugation steps in this study were performed with a centrifuge 5424 R and a fixed angle rotor. To collect the second SEC fraction, 500 μ L of SmartSEC HT isolation buffer was added to each well and the plate was centrifuged again for 2 min at $500 \times g$. Until further use, samples were stored at -80°C . As described previously (Hirschberg et al., 2022), SEC fraction 1 is most suitable for mass spectrometry purposes, therefore, this elution fraction was used for the biomarker study. SEC fraction 2, however, was also collected and stored at -80°C . From this step onwards, a distinction will be made in non-purified CSF (aliquots number two) and CSF-derived EVs (aliquots number one), the latter one being isolated in these steps resulting into two SEC fractions (Figure 2).

2.4 | Protein concentration

For CSF-derived EV samples, total protein content was determined using the NanoOrange Protein Quantitation Kit (Thermo Scientific) following the manufacturer's specifications for both SEC fraction 1 and SEC fraction 2. A standard curve of serially

TABLE 2 Number of samples pooled for the global pool, and for the pool of each diagnostic group.

	Pool	AD	PD	PDD	DLB	HC
Non-purified CSF samples (<i>N</i>)	30	15	15	15	15	15
CSF-derived EV samples (<i>N</i>)	30	15	15	15	15	15

Abbreviations: AD, Alzheimer's disease; CSF, cerebrospinal fluid; DLB, dementia with Lewy bodies; EVs, extracellular vesicles; HC, healthy control; N, number of samples; PD, Parkinson's disease; PDD, Parkinson's disease dementia.

diluted Bovine Serum Albumin (BSA; Thermo Scientific) was used. EV samples were vacuum dried, re-solved in filtered PBS in a volume 1:3 of the dried-down volume and were diluted 1:50 as a final assay concentration. Signals of all samples, in triplicate, were measured on a Synergy HT microplate reader (Agilent Technologies). Values were extrapolated from the BSA curve, using a linear equation, with $r^2 > 0.98$.

For non-purified CSF samples, total protein content was determined using UV absorbance at 280 nm with a NanoDrop spectrophotometer (NanoDrop 2000, method Protein A280, Thermo Scientific). Here, protein sample quantitation was performed by taking 2 μL of each sample and measured in duplicate. Calculations were performed by the NanoDrop operating software (NanoDrop 2000/2000c version 1.3.1).

2.5 | ExoView

To measure the size of tetraspanin positive particles in non-purified CSF, a pool of all conditions was prepared from 30 different samples, as well as a pool for each of the conditions, consisting of 15 samples each (Table 2). To compare tetraspanin presence among the distinct groups, the same pools were prepared with CSF-derived EV samples (after EV isolation) (Table 2). Both types were prepared with samples coming from the same patients, and the same volume of each sample was taken.

ExoView technology was applied using the ExoView Tetraspanin kit (EV-TETRA-C, NanoView Biosciences), which includes the chips, Incubation Solution, antibodies, and Solution A and B. EV fractions were concentrated 18 times with an Amicon Ultra-0.5 Centrifugal Filter Unit (pore size 10 kDa, UFC501024, Merck Millipore) by centrifuging at 4°C for 40 min at 14,000 \times g and then diluted 1:2 in Incubation Solution. Non-purified CSF samples were centrifuged at 4°C for 10 min at 2500 \times g, and the supernatant was diluted 1:5 in Incubation Solution. Of each diluted sample, 35 μL was incubated on a chip (coated with CD9, CD81, CD63 and IgG control antibodies) overnight at room temperature in a 24-well plate without agitation. After four washes under shaking conditions with Solution A, chips were subjected to staining using anti-CD81 CF555, anti-CD9 CF488, anti-CD63 CF647 (each antibody diluted 1:1200 in blocking solution) for one hour without shaking. Subsequently, chips were washed seven times under shaking conditions, twice with Solution A, three times with Solution B, and twice in ultrapure water. All the washing steps were performed automatically with a ExoView CW100 Plate Washer (NanoView Biosciences). Lastly, the chips were dried, scanned by the ExoView R100 reader (NanoView Biosciences) and eventually analysed using the NanoViewer analysis software version 3.1. Statistical analysis was not performed since ExoView was performed on pooled samples and on a limited number of spots, thus no replicates were performed besides the technical replicates based on the three spots on each chip.

2.6 | ZetaView

Particle concentration and size were determined using NTA, with a ZetaView instrument (Particle Metrix, Germany) in fluorescence mode (488-nm laser, 40 mW power), where EVs were bound to CMG (CellMask Green Plasma Membrane Stain, Thermo Scientific). The same CSF-derived EV pool (made of 30 samples) described in Table 2 was used for this experiment. Before measurement, the sample was mixed with CMG (1/100 in filtered PBS, Gibco DPBS powder, no calcium, no magnesium, Fisher Scientific, filtered by a sterile 0.1 μm pore syringe filter, Millipore) and after a one-hour incubation step in the dark at room temperature, EVs with CMG were diluted 1:2 with filtered PBS (sterile 0.1 μm pore syringe filter, Millipore) (final dilution CMG 1:80,000). This is the minimally required dilution since a total volume of at least 800 μL has to be injected in the instrument. Samples that demonstrated less than 25 particles per frame were excluded. In fluorescence mode, only particles emitting fluorescence (normally at a larger wavelength compared to excitation) are detected, as the scattering light (with the same wavelength as the laser) is blocked by a filter with a certain cut-off wavelength (in this case 500 nm, 12 nm larger than the laser wavelength). This filter also blocks some of the fluorescence signal, which is why, prior to analysis, the system was verified with both 100 nm polystyrene latex microbeads (Particle Metrix). FITC-labelled silica beads (Nanocs Inc.) were used to determine the concentration correction factor by comparing the number of measured particles, taking the sensitivity into account, between scatter and fluorescence mode. These beads were used because of their similar scattering characteristics and refractive index. This resulted

TABLE 3 Number of samples analysed by one or more Simoa kits (=Y), and the number of samples reaching the LLOQ (=X), noted as X/Y.

Kit		AD	PD	PDD	DLB	HC
$A\beta_{1-40}$	Non-purified CSF samples (N)	10/10	3/5	5/6	8/10	8/8
	CSF-derived EV samples (N)	0/8	0/5	0/3	0/7	0/8
$A\beta_{1-42}$	Non-purified CSF samples (N)	10/10	3/5	5/6	8/10	8/8
	CSF-derived EV samples (N)	7/8	4/5	1/3	7/7	3/8
T-Tau	Non-purified CSF samples (N)	11/11	5/5	6/6	8/8	8/8
	CSF-derived EV samples (N)	8/8	5/5	3/3	7/7	8/8
pTau181	Non-purified CSF samples (N)	6/6	–	–	6/6	6/6
	CSF-derived EV samples (N)	5/9	–	–	3/8	3/7
NfL	Non-purified CSF samples (N)	11/11	5/5	6/6	8/8	8/8

Abbreviations: AD, Alzheimer's disease; $A\beta$, β -amyloid; CSF, cerebrospinal fluid; DLB, dementia with Lewy bodies; EVs, extracellular vesicles; HC, healthy control; N; NfL, neurofilament light; number of samples; PD, Parkinson's disease; PDD, Parkinson's disease dementia; pTau181, tau phosphorylated at threonine-181; T-Tau, total tau.

in a correction factor of 1.3, meaning the number of particles were underestimated in fluorescence mode by 23% compared to scatter mode.

For each measurement, two cycles of each 11 positions were performed, with a frame rate of 30. Settings were kept constant for all samples (focus: autofocus; camera sensitivity: 80.0 (scatter mode) or 97 (fluorescence mode); shutter: 100.0; temperature: 22.0°C). The videos were analysed by the ZetaView software version 8.05.11 SP2 (minimum brightness: 30, minimum particle size: 10, maximum particle size: 1000). More characterisation data of CSF-derived EVs with the SmartSEC kit was published in 2022 (Hirschberg et al., 2022).

2.7 | Simoa

In a sub-cohort of both the non-purified CSF samples and the CSF-derived EV samples (after EV isolation) (Table 3), $A\beta$, tau and neurofilament light polypeptide (NfL) were measured by commercially available immunoassays. $A\beta_{1-40}$, $A\beta_{1-42}$, T-Tau (kit Neurology 3-Plex A Advantage Kit, Quanterix, ref. 101995), pTau181 (kit pTau181 Advantage V2.1 Kit, Quanterix, ref. 10411), and NfL (kit NF-LIGHT V2 Advantage Kit, Quanterix, ref. 104073) were quantified with an SR-X instrument (Quanterix) at the Sant Pau Biomedical Research Institute, Barcelona, Spain. Non-purified CSF samples were diluted 1:100 for the Neurology 3-plex kit, 1:10 for pTau181, and 1:80 for NfL measurements. EV samples were first lysed with M-PER (Thermo Scientific, ref. 78501), mechanically with 29-gauge syringes (SG SH lab solutions, ref. UNI4112), by two 45-s sonication steps, and by two F/T cycli. Then they were diluted 1:10 before using the Neurology 3-plex kit and the pTau181 kit. NfL was not measured in CSF-derived EV samples since the test measurements were below the limit of detection (LOD).

For the determination of the lower limit of quantification (LLOQ), the calibrator was analysed in duplicates at concentrations between 0.673 and 136 pg/mL for $A\beta_{1-40}$, 0.225 and 53.1 pg/mL for $A\beta_{1-42}$, 0.143 and 73.1 pg/mL for T-Tau, 2.07 pg/mL and 423 pg/mL for pTau181, and 0.403 and 365 pg/mL for NfL.

2.8 | Statistical analysis

Statistical analysis was performed using Graphpad 9.5.1, with p -value <0.05 as a significance index. All variables in group-wise comparisons were submitted to Shapiro-Wilk tests for normality and analysed using one-way ANOVA followed by the Tukey post-test (parametric data) or Kruskal–Wallis followed by Dunn's post hoc-test (non-parametric data). Associations between biomarkers were tested with a two-tailed Spearman's Rank or Pearson's correlation analysis, with a confidence interval of 95%. This was done on protein and peptide concentration measurements (non-parametric data) and Simoa data (both parametric and non-parametric data).

2.9 | LC-MS/MS sample preparation

For LC-MS/MS sample preparation, the cohort was divided into 18 different sample batches using block randomisation (Burger et al., 2021) (Table S1). To gain insight into quality and batch variances of the LC-MS/MS measurements, a reference sample was

prepared. For this cause, a pooled sample was prepared, containing different samples of all experimental groups (see Table S2 and Table S3). For CSF-derived EV samples, as there was a limitation in available material, 63 samples of the cohort were selected with the highest protein concentration. Of each of those proteins, 0.75 μg was taken, pooled, and used as reference sample. For the non-purified CSF pooled reference sample, 20 μL of all samples out of batch 1 and 2 was used. Pooled samples were stored at -80°C until sample preparation.

2.10 | Protein extraction and S-trap digestions

Each sample was digested in an S-trap micro spin column (Protifi, ref. CO2-micro) (Figure 1c) according to the manufacturer's instructions. First, 0.75 μg of protein of each CSF-EV derived sample was concentrated in a vacuum dryer (Speedvac SPD1010, Thermo Scientific) and placed in a sonication bath (Branson 3510, Marshall Scientific) for 20 min with a final concentration of 5% SDS (Sigma-Aldrich, ref. L3771). For non-purified CSF samples, 10 μL was taken and the same steps were applied.

Proteins were reduced with a final concentration of 10 mM DTT (Sigma, ref. D0632) for 30 min at 55°C with 450 rpm in a Thermomixer C (Eppendorf), followed by an alkylation step with a final concentration of 20 mM iodoacetamide (Sigma, ref. I1149) for at least 30 min at room temperature in the dark. The alkylated proteins were acidified by adding phosphoric acid (Biosolve, ref. 161605) to a final concentration of 2.7% and mixed with six volumes of binding buffer (90% methanol, Biosolve, ref. 136841; final concentration of 100 mM TEAB, Sigma, ref. T7408). After vortexing, the solution was loaded onto the S-trap filter and centrifuged at $4000 \times g$ for 30 s. After all sample was loaded, three washing steps with each time 150 μL of the binding buffer were performed followed by a centrifugation step of $4000 \times g$ for 30 s, ending with an additional centrifugation step of $4000 \times g$ for 1 min. An overnight digestion with 0.5 μg (CSF-EV derived samples) or 1.0 μg (non-purified CSF samples) Trypsin Platinum (Promega, ref. VA9000) diluted in 20 μL 50 mM TEAB per sample was performed at 37°C in a humid environment to limit evaporation. Finally, peptides were eluted stepwise with three elution buffers at a volume of 40 μL each, including 50 mM TEAB in water, 0.2% formic acid (Biosolve, ref. 069141A8) in water and 50% acetonitrile (Biosolve, ref. 01204101)/0.1% formic acid in water. The peptide solutions were pooled, speed-vacuum dried, and subsequently stored at -20°C . All water used in this protocol was HPLC-graded water (Biosolve, ref. 232141B1).

2.11 | LC-MS/MS analysis

All dry CSF-derived EV samples were resuspended in 20 μL of Solvent A (0.1% formic acid in water, Biosolve, ref. 23244102), and all material was used for further steps. Dry non-purified CSF samples were resuspended in 22 μL Solvent A. With 2 μL of each sample, the peptide concentration was measured using the NanoDrop spectrophotometer, and 0.3 μg of peptide was taken to load onto the column.

Before injecting all samples into the mass spectrometer, samples were loaded on Evotips Pure (Evosep, EV2013) according to manufacturer's instructions (Evotip Pure sample loading protocol, downloaded 13.06.2022). In short, Evotips Pure were washed with Solvent B (0.1% formic acid in acetonitrile, Biosolve, ref. 01930602), and conditioned in 1-propanol (Biosolve, ref. 16360602). After equilibrating with Solvent A, the required volume of peptides was loaded onto the tip. Following a centrifugation step of $800 \times g$ for 1 min, tips were washed with Solvent A and additional Solvent A was added to avoid drying of the tip. Finally, 1 pmol/peptide from the Retention Time standardisation kit PROCAL (JPT, ref. RTK-1-10 pmol) (Zolg et al., 2017) was added to all samples. A peptide mixture from a HeLa cell culture was used as QC sample at the beginning and end of every batch, and a sample with GFP (Protea biosciences, MorganDown, WV) was run every three samples.

The peptide samples were separated on a Evosep One (Evosep, Figure 1d), fitted with an ReproSil-Pur C18 Endurance column (15 cm, 1.9 μm , 150 μm , Evosep, EV1113). The pre-programmed Evosep 30 SPD method was used. The column was online with a timsTOF Pro (Figure 1d) operating in positive ion mode, coupled with a CaptiveSpray ion source (both from Bruker Daltonics GmbH, Bremen). The timsTOF Pro was calibrated according to the manufacturer's guidelines. The temperature of the ion transfer capillary was 180°C . The Parallel Accumulation-Serial Fragmentation (PASEF) DDA method was used to select precursor ions for fragmentation with 1 TIMS-MS scan and 10 PASEF MS/MS scans, as described by Meier et al. (2018). The TIMS-MS survey scan was acquired between 0.70–1.45 V s/cm² and 100–1700 m/z with a ramp time of 100 ms. The 10 PASEF scans contained on average 12 MS/MS scans per PASEF scan with a collision energy of 10 eV. Precursor ions with 1–5 charges were selected with the target value set to 20,000 a.u and intensity threshold to 2500 a.u. Precursors were dynamically excluded for 0.4 s. The timsTOF Pro was controlled by the OtofControl 5.1 software (Bruker Daltonik GmbH). 10 PASEF scans contained on average 12 MS/MS scans per PASEF scan. Raw data was analysed with the DataAnalysis 5.1 software (Bruker Daltonik).

2.12 | Peptide identification

A peptide search was performed on a selection of 50 CSF-derived EV samples. MaxQuant version 2.2.0.0 (Max-Planck Institute, Germany) (Cox & Mann, 2008), with the Andromeda search engine, was used to perform database searches against the database Uniprot Human (Proteome ID: UP000005640, downloaded on 30th January 2020), with a protein FDR of 1%. Methionine oxidation and serine, threonine and tyrosine phosphorylation were set as variable modifications and cysteine carbamidomethylation as a fixed modification. During the search, the trypsin digest was allowed to have two missed cleavage sites. Identifications were transferred between runs with the match-between-runs setting. The MaxQuant .msms output file was used to generate a spectral library with BiblioSpec implemented in the Skyline environment. Here, peptides shared between multiple protein groups were removed and only protein groups with minimally two peptides were considered. The raw data of all other 199 CSF-EV derived samples (249 total samples minus the 50 samples already run on MaxQuant) were imported in this spectral library. The same was done for non-purified CSF samples: a selection of 50 samples was run on MaxQuant, with which a spectral library in Skyline was made for the other 198 samples. The use of such spectral library helps avoiding missing values, an issue often encountered in label-free quantitative proteomics.

2.13 | Differential analysis

Further data analysis was performed in R version 4.3.1 (Posit). The peptide intensities acquired by Skyline were log₂-transformed, filtered for maximum 50% missing values, normalised using the quantile method, and summarised into protein expression values. Package limma (version 3.52.4) from Bioconductor was used for the actual differential analysis (Phipson et al., 2016). Proteins were considered differentially expressed if the Benjamini-Hochberg-adjusted *p*-value was lower than 0.05 (FDR 5%) and the absolute log₂ fold change (LogFC) was higher than 1.

2.14 | GO enrichment

DAVID Bioinformatics Resources 2021 (<https://david.ncifcrf.gov>) was used to perform GO (gene ontology) analysis. The whole proteome background was retrieved from the database Uniprot Human (Proteome ID: UP000005640, downloaded on 30th January 2020).

2.15 | Network analysis

A network analysis was performed using STRING version 11.5. STRING is a database of known and predicted protein-protein interactions. Its search tool was used for the retrieval of interacting genes within statistically significant differentially expressed proteins from non-purified CSF samples and from CSF-derived EV samples. After entering accession numbers, Markov Clustering (MCL) was performed with the default value of inflation parameter (3). Disconnected nodes were hidden, and only highest confidence interactions were shown with a minimum required interaction score of 0.9000 (Szklarczyk et al., 2023).

3 | RESULTS

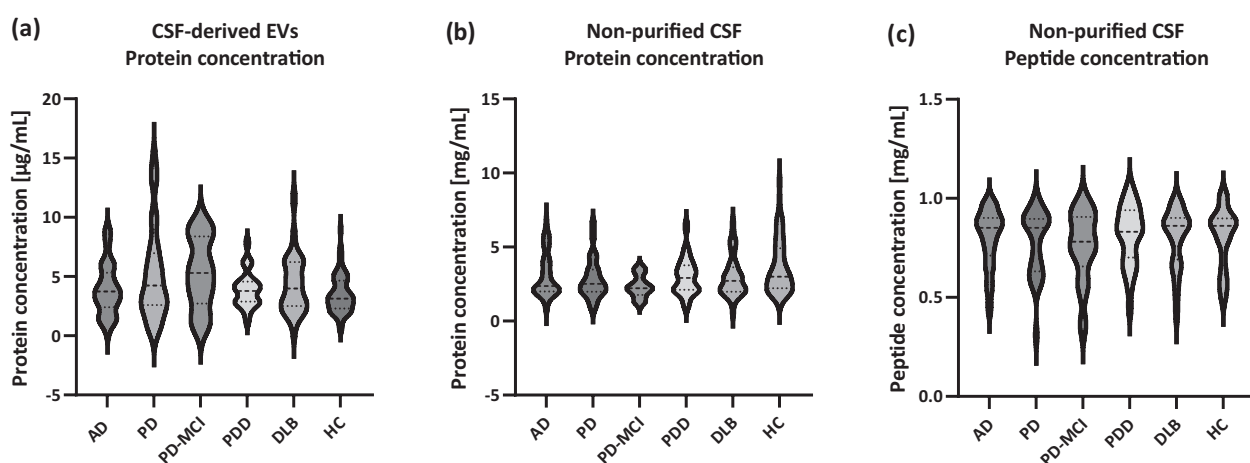
3.1 | Protein and peptide concentrations

On average, the protein concentration of CSF-derived EVs was 4.57 $\mu\text{g}/\text{mL}$. Of each sample, 0.75 μg was allocated for protein extraction and peptide digestion (i.e., LC-MS/MS sample preparation). The protein concentration of non-purified CSF was about 1000 times higher, with an average of 4.19 mg/mL . Since 20 μL of these samples was taken for LC-MS/MS sample preparation, on average 41.94 μg of protein was taken. Measurements at peptide level resulted in an average concentration of 0.81 mg/mL , which means that on average 17.79 μg of peptide was retrieved after sample preparation, or 42.42% of the initial protein material. The descriptive statistics can be found in Table 4.

Protein concentration of CSF-derived EVs and non-purified CSF did not correlate significantly according to a Spearman test ($\rho = 0.106$, p -value = 0.095). However, as expected, there was a significant correlation between the protein and peptide concentrations of non-purified CSF ($\rho = 0.241$, p -value = 7.322E-005). This shows the reproducibility of the sample preparation protocol and the amount of material lost. Between the different phenotypes, no significant difference was measured for protein or peptide measurement in both the CSF-derived EV samples and the non-purified CSF (Figure 3). These statistics were performed both

TABLE 4 Descriptive statistics of protein and peptide concentration measurements.

Sample type	CSF-derived EVs	Non-purified CSF	
	Protein concentration ($\mu\text{g/mL}$)	Protein concentration (mg/mg)	Peptide concentration (mg/mL)
Minimum	0.10	0.54	0.31
25% Percentile	2.61	2.11	0.72
Median	3.74	2.93	0.86
75% Percentile	5.84	4.51	0.91
Maximum	22.44	27.86	1.06
Mean	4.571	4.194	0.8085
Std. Deviation	3.377	3.933	0.1487
Std. Error of Mean	0.1966	0.2309	0.008660
Coefficient of variation	73.87%	93.77%	18.40%

**FIGURE 3** Violin plots of protein and peptide concentration comparisons between different phenotypes, after removing outliers (ROUT, $Q = 1\%$). AD, Alzheimer's disease; CSF, cerebrospinal fluid; DLB, dementia with Lewy bodies; EVs, extracellular vesicles; HC, healthy controls; PD, Parkinson's disease; PD-MCI, Parkinson's disease with mild cognitive impairment; PDD, Parkinson's disease dementia.

with and without removing outliers (ROUT method, $Q = 1\%$).

Seyfert et al. described a similar average CSF total protein concentration of 4.00 mg/mL in controls, of which 2.23 mg/mL albumin and 0.24 mg/mL IgG. Furthermore, they observed a positive correlation between albumin quotient and age (Seyfert et al., 2002). Comparing non-purified CSF protein concentrations (median of 2.93 mg/mL) with CSF-derived EV protein concentrations (median of 3.74 $\mu\text{g/mL}$) supports the notion that the SmartSEC kit indeed efficiently removes abundant proteins, such as albumin, as previously demonstrated (Hirschberg et al., 2022).

3.2 | ExoView

The objective of analysing non-purified CSF samples on the ExoView platform was to obtain a particle size distribution. However, since the mean size of CD63, CD81 and CD9 captured particles was 54 nm ($SD = 5$), 55 nm ($SD = 6$) and 56 nm ($SD = 7$), respectively, and the minimum measurable size on the instrument is 50 nm according to the manufacturer (Deng et al., 2022), it is probable that many particles were not accounted for in this measurement. Possibly due to aforementioned issue, there was no noticeable variation in particle size among the different phenotypes (Figure 4a). At the same time as this scatter analysis, CD63 double positive particles in fluorescence mode were counted (Figure 4b). Here, AD appeared to have a higher number of particles compared to other phenotypes. Similarly, in the fluorescence experiment conducted with CSF-derived EVs, DLB exhibited a higher number of particles compared to other phenotypes (Figure 5b). For these samples, the total number of particles captured by CD63, CD81 and CD9 was also counted, revealing that CD63 captured most particles, and that the DLB pool consisted of more CD9 captured particles than the other groups. In contrast, in the case of non-purified CSF, this comparison was not carried

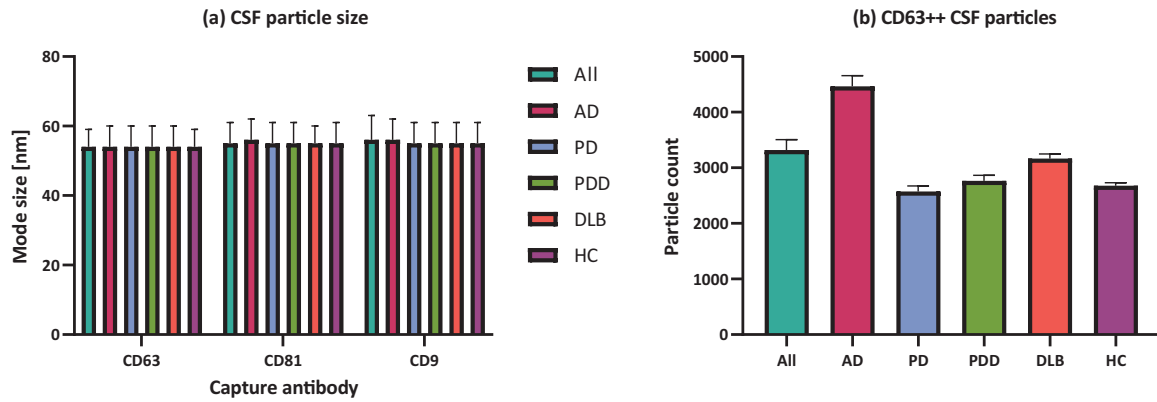


FIGURE 4 Non-purified CSF ExoView results. (a) Mean particle size and SD of the ExoView in scatter mode, for the particles captured by the three different capture antibodies (CD63, CD81, CD9), per diagnostic group. (b) Counted number of particles double positive for CD63 and their SD. AD, Alzheimer's disease; CSF, cerebrospinal fluid; DLB, dementia with Lewy bodies; HC, healthy control; PD, Parkinson's disease; PDD, Parkinson's disease dementia.

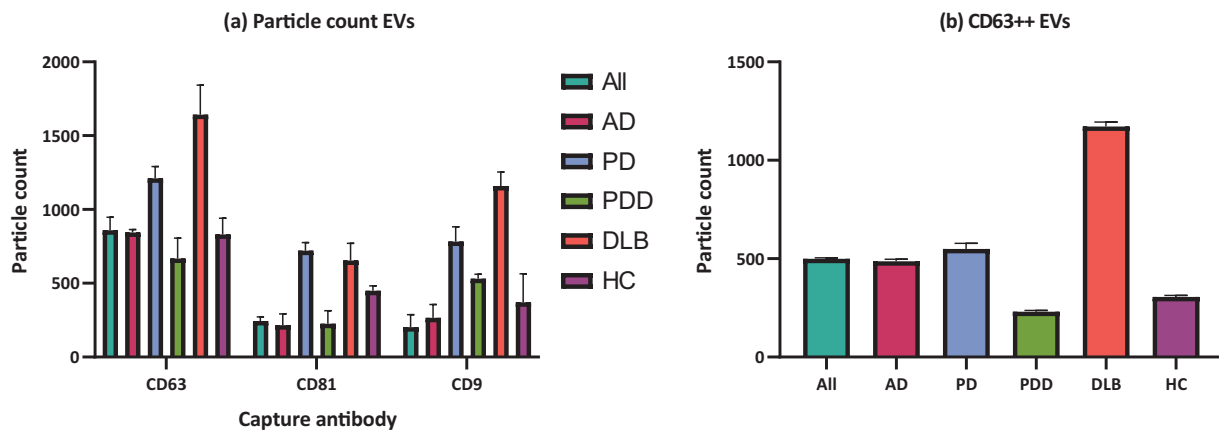


FIGURE 5 CSF-derived EVs ExoView results. (a) Total number particles counted on the three capture antibodies (CD63, CD81, CD9) per diagnostic group, by fluorescence. (b) Counted number of particles double positive for CD63. AD, Alzheimer's disease; DLB, dementia with Lewy bodies; EVs, extracellular vesicles; HC, healthy control; PD, Parkinson's disease; PDD, Parkinson's disease dementia.

out, except for CD63++ particles, since other tetraspanins oversaturated the chips. Interestingly, in these samples, CD63 was the least detected protein among the three tetraspanins measured.

3.3 | ZetaView

In the CSF-derived EV pooled sample, a concentration of 1.1×10^8 particles per millilitre (dilution factor and correction factor considered) was observed, and a median size of 106.5 nm in a measurement where, in average, 112 particles were measured per frame.

3.4 | Simoa

For NfL and pTau181, samples were split in groups AD, DLB or PDD, and HC. For non-purified CSF samples, NfL was significantly higher in DLB/PDD than HC (p -value = 0.0459) and after removing two outliers, AD samples had significantly higher NfL concentrations than HC likewise (p -value = 0.0384) (Figure 6). For pTau181, no significant differences were found in these samples (p -values range between 0.1633 and 0.8639). Since more non-purified CSF samples were tested on the Neurology 3-plex kit, more groups were included for these analytes (namely AD, PD, PDD, DLB, HC). In these experiments, $A\beta_{1-42}$ was significantly lower in AD than in PDD (p -value = 0.0219) and HC (p -value = 0.0176) (Figure 6). $A\beta_{1-40}$ was marginally lower in AD than PDD

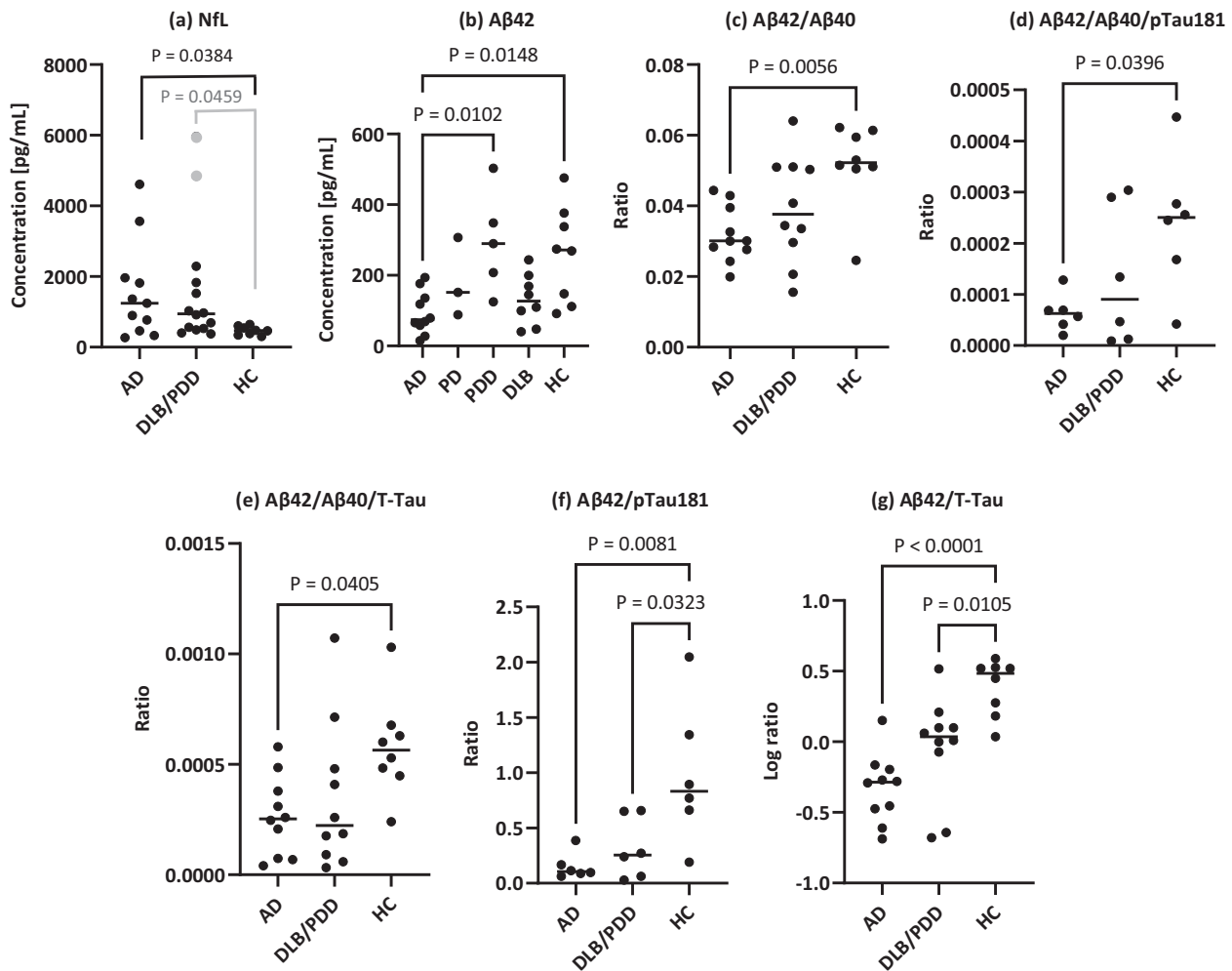


FIGURE 6 Overview of the significant differences between mean concentrations of analytes in non-purified CSF, as measured by Simoa. A significant difference is observed for (a) NfL concentrations, between AD and HC using Kruskal–Wallis (no normal distribution). When removing two outliers (in grey), normal distribution was achieved, and one-way ANOVA highlighted a significant difference between DLB/PDD and HC; (b) $A\beta_{1-42}$ concentrations; (c) the ratio of $A\beta_{1-42}$ on $A\beta_{1-40}$; (d) the ratio of $A\beta_{1-42}$ on $A\beta_{1-40}$ on pTau181; (e) the ratio of $A\beta_{1-42}$ on $A\beta_{1-40}$ on T-Tau; (f) the ratio of $A\beta_{1-42}$ on pTau181; (g) the ratio of $A\beta_{1-42}$ on T-Tau. $A\beta$, β -amyloid; AD, Alzheimer's disease; DLB, dementia with Lewy bodies; HC, healthy controls; NfL, neurofilament light; PDD, Parkinson's disease dementia; pTau181, tau phosphorylated at threonine-181; T-Tau, total tau.

TABLE 5 Particle size distribution and concentration.

X10 size	90.4 nm
X50 size	169.5 nm
X90 size	215.9 nm
Median size	106.5 nm
Concentration	1.1E+8 particles/mL
Average counted particles per frame	112

(p -value = 0.0618). Figure 6 shows the significant differences between the phenotypes for the calculated ratios of the analytes. Ratios pTau181/NfL and pTau181/T-Tau (not shown in the Figure) were also calculated, but did not show any significance.

For CSF-derived EVs, no significant differences were found for pTau181, T-Tau, $A\beta_{1-40}$, $A\beta_{1-42}$ or any of the calculated ratios. As seen when comparing Tables 3 and 6, not all samples reached the LLOQ in the three used kits. Therefore, not as many values were retrieved for these samples as for the non-purified CSF.

For all biomarkers summed up in Table 6, correlation was checked between non-purified CSF samples and CSF-derived EV samples. However, no significant correlations were found following a two-tailed Spearman test. It should be noted that the

TABLE 6 Overview of the mean concentrations \pm standard deviations of NfL, pTau181, A β_{1-40} , A β_{1-42} , T-Tau and their ratios, as measured by Simoa.

Non-purified CSF			
Biomarker/ratio	AD (pg/mL) (N)	DLB/PDD (pg/mL) (N)	HC (pg/mL) (N)
NfL	1572 \pm 1384 (11) ^a	1602 \pm 1721 (14) ^c	469.8 \pm 121.7 (8) ^{abc}
pTau181	671.6 \pm 382.5 (6)	813.4 \pm 709.8 (6)	283.7 \pm 156.3 (6)
A β_{1-40}	3,393 \pm 2,590 (10)	5,305 \pm 3,988 (13)	5,040 \pm 2,158 (8)
A β_{1-42}	93.9 \pm 60.16 (10) ^{a,b}	194.5 \pm 129.1 (13) ^b	260.5 \pm 136 (8) ^a
T-Tau	197.3 \pm 149.5 (10)	163.5 \pm 165.3 (13)	94.7 \pm 20.5 (8)
A β_{1-42} /A β_{1-40}	0.032 \pm 0.008 (10) ^{aa}	0.039 \pm 0.015 (10)	0.052 \pm 0.012 (8) ^{aa}
pTau181/NfL	1.005 \pm 1.029 (6)	1.058 \pm 0.652 (6)	0.631 \pm 0.234 (6)
pTau181/T-Tau	4.465 \pm 1.037 (6)	3.749 \pm 1.814 (6)	2.986 \pm 1.373 (6)
A β_{1-42} /A β_{1-40} /pTau181	6.409E-005 \pm 3.658E-005 (6) ^a	1.328E-004 \pm 1.35E-004 (6)	2.392E-004 \pm 1.332E-004 (6) ^a
A β_{1-42} /A β_{1-40} /T-Tau	2.651E-004 \pm 1.800E-004 (10) ^a	3.479E-004 \pm 3.320E-004 (10)	5.800E-004 \pm 2.267E-004 (8) ^a
A β_{1-42} /pTau181	0.153 \pm 0.120 (6) ^{aa}	0.319 \pm 0.277 (6) ^c	0.985 \pm 0.640 (6) ^{aa,c}
A β_{1-42} /T-Tau	0.545 \pm 0.346 (10) ^{aaaa}	1.187 \pm 0.859 (10) ^c	2.644 \pm 1.013 (8) ^{aaaa,c}
CSF-derived EVs			
Biomarker/ratio	AD (pg/mL) (N)	DLB/PDD (pg/mL) (N)	HC (pg/mL) (N)
pTau181	0.358 \pm 0.262 (5)	0.204 (1)	0.090 \pm 0.109 (3)
A β_{1-42}	0.790 \pm 0.244 (7)	0.886 \pm 0.543 (5)	0.897 \pm 0.582 (3)
T-Tau	0.233 \pm 0.098 (8)	0.1905 \pm 0.112 (10)	0.147 \pm 0.091 (8)
A β_{1-42} /T-Tau	3.856 \pm 2.055 (7)	4.816 \pm 4.628 (5)	3.983 \pm 1.846 (3)

The number of samples measured is indicated within brackets. Significant differences with p -value <0.05 , p -value <0.01 , p -value <0.001 and p -value <0.0001 are respectively indicated with one, two, three and four repeated superscript letters; the following letters are used: a = AD vs. HC, b = AD vs. DLB/PDD, c = DLB/PDD vs. HC.

Abbreviations: A β , β -amyloid; AD, Alzheimer's disease; CSF, cerebrospinal fluid; DLB, dementia with Lewy bodies; EVs, extracellular vesicles; HC, healthy controls; N, number of samples included; NfL, neurofilament light; PDD, Parkinson's disease dementia; pTau181, tau phosphorylated at threonine-181; T-Tau, total tau.

number of paired samples used for these tests was limited. The different analytes measured in non-purified CSF samples did show significant correlations among themselves: NfL and pTau181 ($\rho = 0.461$, p -value = 0.047, $N = 19$), NfL and A $\beta_{1-42}/_{1-40}$ ($\rho = -0.372$, p -value = 0.030, $N = 34$), pTau181 and A $\beta_{1-42}/_{1-40}$ ($\rho = -0.909$, p -value = 7.323E-008, $N = 19$), pTau181 and T-Tau ($\rho = 0.791$, p -value = 5.473E-005, $N = 19$), A β_{1-42} and A $\beta_{1-42}/_{1-40}$ ($\rho = 0.347$, p -value = 0.044, $N = 34$), A $\beta_{1-42}/_{1-40}$ and T-Tau ($\rho = -0.591$, p -value = 2.299E-004, $N = 34$) (Figure 7).

3.5 | LC-MS/MS

The number of protein groups identified and quantified was 350 in non-purified CSF, whereas this number increased to 658 protein groups for CSF-derived EVs. Of these identifications, 147 protein groups overlapped between both datasets. To check if age and storage time were confounders of the LC-MS/MS data, linear regression was performed per group and was shown non-significant for most proteins (p -values can be found per group for all biomarker candidates in the supplementary PDF, for both non-purified CSF and CSF-derived EVs).

All included groups (HC, AD, PD, PD-MCI, PDD, DLB) were compared, resulting in 15 comparisons for each protein, per sample type. For non-purified CSF, 169 statistically significant proteins were detected over all groups in total (supplementary Excel, sheet 'non-purified CSF'). Only for AD versus PD-MCI and PD-MCI versus PDD, no differential proteins were found. For CSF-derived EVs, 276 statistically significant proteins were detected over all groups (supplementary Excel, sheet 'CSF-derived EVs'). Here, for AD versus PD-MCI, AD versus PDD, PD-MCI versus PDD and PD versus PD-MCI, no differential proteins were discovered. Between both sample types, almost no overlap was found in differential proteins (Figures S1 and S2; supplementary Excel, sheet 'Venn').

To investigate the characteristics of the CSF-derived EV proteome and non-purified CSF proteome, we employed DAVID using a human proteome reference list. Among the overrepresented GO classes, in CSF-derived EVs, we found overrepresentation of entries related to ribosomes, extracellular space, melanosome, secretory granule lumen, ficolin-1-rich granule lumen, cytoplasm, extracellular region, focal adhesion, cytosol and extracellular exosomes (sorted by p -value). For the non-purified CSF, we found entries related to melanosomes, ribosomes, cytosol, blood microparticles, cell surface, endoplasmic reticulum lumen,

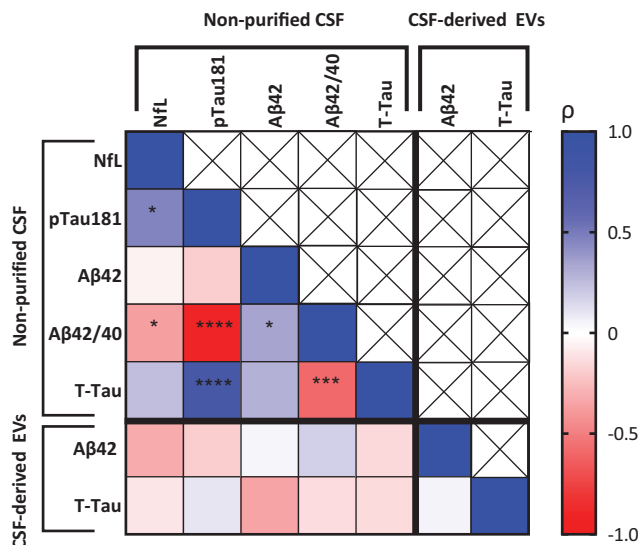


FIGURE 7 Heatmap of two-tailed Spearman correlation test between the analytes measured by Simoa in both non-purified CSF and CSF-derived EVs. Spearman's ρ is illustrated according to a gradient scale from blue to red (as shown on the right of the Figure), and significant p -values are indicated by asterisk: p -value < 0.05 (*), p -value < 0.01 (**), p -value < 0.001 (***), p -value < 0.0001 (****). A β , β -amyloid; CSF, cerebrospinal fluid; EVs, extracellular vesicles; Nfl, neurofilament light; pTau181, tau phosphorylated at threonine-181; T-Tau, total tau.

extracellular matrix, (external side of) plasma membrane, circulating immunoglobulin complex. In regard to the cellular component, almost half of CSF-derived EV proteins were related to the cytoplasm, while for non-purified CSF about half were secreted. For both sample types, enrichment between all detected proteins and differential proteins were comparable (supplementary Excel sheet 'DAVID').

3.6 | Selection of biomarkers

To identify the most promising markers out of these lists of differential proteins, a selection process was carried out based on the comparisons where the protein was significant. The first selection focused on markers for neurodegeneration in general (see Table 7 'neurodegeneration'). Here, the proteins were selected that showed a significant result between comparison HC versus AD, HC versus DLB, HC versus PD, HC versus PD-MCI and HC versus PDD. Among non-purified CSF differential proteins, two markers were selected, while 33 met the criteria among CSF-derived EV proteins.

For AD markers (see Table 7, Figures 8 and 9 'AD'), the selection aimed for markers that could make a distinction between HC versus AD and/or AD versus DLB, while excluding those associated with non-AD diseases. This resulted in 10 potential markers in non-purified CSF and four in CSF-derived EVs.

To identify DLB- specific markers (see Table 7, Figures 8 and 9 'DLB'), hypothesizing that this is a disease that pathophysiologically differs from PDD, markers were selected if they differentiated HC versus DLB and AD versus DLB, while not differentiating between non-DLB diseases. This led to the selection of 15 DLB non-purified CSF markers and nine DLB CSF-derived EV markers.

For PD (see Table 7, Figures 8 and 9 'PD'), the criteria were to differentiate between HC versus PD and PD versus PDD, and not for non-PD diseases. In this case, four non-purified CSF markers were noted and 13 CSF-derived EV markers. For PDD (see Table 7, Figures 8 and 9 'PDD'), hypothesizing that this is a different disease from DLB, the focus was on markers that differentiated HC versus PDD and AD versus PDD or DLB versus PDD, while excluding markers associated with non-PD or non-PDD diseases. Five non-purified CSF markers were selected, and three for CSF-derived EVs. These markers did not appear in the MCI stage of PD. Markers that could potentially measure dementia already in the PD-MCI stage, were selected based on differentiation between both HC versus PD-MCI and HC versus PDD (see Table 7, Figures 8 and 9 'PDMCI-PDD'): three identifications for non-purified CSF and five for CSF-derived EVs. Lastly, hypothesizing that DLB and PDD are actually one and the same disease, a selection was made based on markers that showed significance for HC versus the PD continuum and HC versus DLB, while excluding proteins that could also differentiate AD (see Table 7, Figures 8 and 9 'PDMCI-DLB-PDD').

In Figures 8 and 9, all proteins mentioned in Table 7 are illustrated with their LogFC value and according p -value between all group comparisons. Proteins were considered differentially expressed if the Benjamini-Hochberg-adjusted p -value was lower than 0.05 and the absolute LogFC was higher than 1. Based on this, as described above, the selection of biomarkers was performed for each of the diseases.

TABLE 7 Selection of most promising protein biomarker candidates (annotated with their gene name) for both non-purified CSF and CSF-derived EVs. An asterisk (*) highlights the proteins that showed up in the network analysis as well, as expanded upon in the supplementary data (Figure S3, Figure 4, Tables 4 and 5). Neurodegeneration: Differentiate HC vs. AD, HC vs. DLB, HC vs. PD, HC vs. PD-MCI, and HC vs. PDD. AD: Differentiated HC vs. AD and/or AD vs. DLB, and not non-AD diseases. DLB: Differentiated HC vs. DLB and AD vs. DLB, and not non-DLB diseases. PD: Differentiated HC vs PD and PD vs. PDD, and not non-PD diseases. PDD: Differentiated HC vs. PDD and AD vs. PDD or DLB vs. PDD and not non-PD or non-PDD diseases. PDMCI-PDD: Differentiated HC vs. PD-MCI and HC vs. PDD. PDMCI-DLB-PDD: Differentiated HC vs. the PD continuum and HC vs. DLB.

	Non-purified CSF	CSF-derived EVs
Neurodegeneration	IGHV3-48, SYNRG (N = 2)	TAGLN, KRT8, SRI, NUTF2, SELENBP1, RPS18*, IGLC7, TMSB4X*, SF3A1*, HRNRNPK, STMN, NCL*, RPL7*, ACIN1, RPL31*, COL28A1, FABP6*, EIF3D*, PPT1, RPL22*, TRA2B*, SUMO2*, MLF2, ST13P4, MESD, CCT5*, S100A6, PSMD2*, HMGB1P1, ACLY*, MYO6*, PSMA7*, RNASE4 (N = 33)
AD	IGKV3D-15, CA3, SORCS3, MYH9*, TUBB2B, GALNT1, CALML5, SMOCL1, SPINT2*, BAMBI* (N = 10)	CFHR2, EDF1, PLA2G4E, ARLU1 (N = 4)
DLB	PLXDC2, SHISA5, CPLANE1, PCDH9, C1RL, SERPINB4*, ACTC1, MGP, CD81, IGHV3-30-5, PRKCSH*, SLPI, F2R*, IGHV2-70D, SPOCK1 (N = 15)	SAMD9, SIRPA, PREX1*, LDHA, TCOF1, EPHB1, RBICC1, KRT40, KRT38 (N = 9)
PD	EPHB6*, KRT8, EPB42, CENPE (N = 4)	RALB, POR, SMPD3, MAPT*, DDX6*, ILK*, OGN*, CTSS*, PPP1CC*, FLIL, IGKV1-8, SHMT1, RPL35A* (N = 13)
PDD	SNCA, MASPI*, PLD4, PTPRS, CADM2 (N = 5)	EHD2, ACTBL2, SLIRP (N = 3)
PDMCI-PDD	HEG1, MOG, PNP* (N = 3)	XIRP2, HP*, IGG1, SORL1*, TF (N = 5)
PDMCI-DLB-PDD	WFIKKN2, PTPRN2 (N = 2)	TGM5, IGLC1, ALB* (N = 3)

Abbreviations: AD, Alzheimer's disease; DLB, dementia with Lewy bodies; N, number of proteins; PD, Parkinson's disease; PDD, Parkinson's disease dementia; PDMCI, Parkinson's disease with mild cognitive impairment.

4 | DISCUSSION

In order to identify biomarker candidates that have high potential for differential diagnosis, or that potentially provide targets for novel or repurposed pharmacotherapeutics, we compared the non-purified CSF and CSF-derived EV proteome of clinically very well phenotyped AD, PD, PD-MCI, PDD and DLB patients, analysed by label-free mass spectrometry. That the patient cohort was well-phenotyped was demonstrated by the fact that the clinical diagnosis was confirmed by *post-mortem* neuropathological and immunohistochemical evaluation of the brain in 25 cases.

First, the protein extractions of the included samples were characterised. Although measured CSF protein concentrations are often lower than measured in this study (Wuschek et al., 2019; Yoshihara et al., 2021), extensive individual variability has been reported previously (Asgari et al., 2017). In order to check if there was a correlation between sample storage time and protein concentration, linear regression was performed. The linear regression slope was shown non-significant for sample storage time and the protein concentration after EV isolation. A second characterisation part was the sizing of the particles. CSF-derived EV particle sizes as measured by ZetaView, resulted in a median size of 106.5 nm, which is significantly larger than the non-purified CSF tetraspanin containing particles measured by ExoView in this study (mean of 54–56 nm, depending on the capture antibody). Unfortunately, attempts to size CSF-derived EVs on the ExoView were unsuccessful, as measurements were below the LOD. Therefore, a comparison between ExoView and NTA was not possible for CSF-derived EV samples. Measuring non-purified CSF with ZetaView, on the other hand, is not meaningful, as the presence of other lipid-membrane contaminating particles would contribute to the fluorescent signal greatly. Notably, some other studies did show that particles seemed smaller using ExoView than NTA such as ZetaView or Nanosight and that ExoView sizes seemed closer to TEM sizes (Bachurski et al., 2019; Comfort et al., 2021).

Next, a more in-depth analysis of the protein content was performed to offer biological information of the diagnoses and of the cargo that CSF-derived EVs carry. On the one hand, targeted proteomics was applied to detect known clinically relevant proteins. NfL, for instance, is a cytoskeletal protein specific to neurons and predominantly present in myelinated axons. Damage to axons leads to the release of NfL into CSF and subsequently into the bloodstream. Elevated levels of NfL are indicative of severe cerebral axonal degeneration and have been associated with various neurodegenerative disorders, including AD (Mattsson et al., 2019), and PD (Hansson et al., 2017). In our study, NfL levels in CSF-derived EVs could not be measured, but non-purified AD CSF NfL levels were significantly higher than HC. After removal of outliers, DLB/PDD scored higher than HC as well. This was expected, since literature indicates that CSF NfL is elevated in AD and DLB compared to HC (Delaby et al., 2020). Most studies

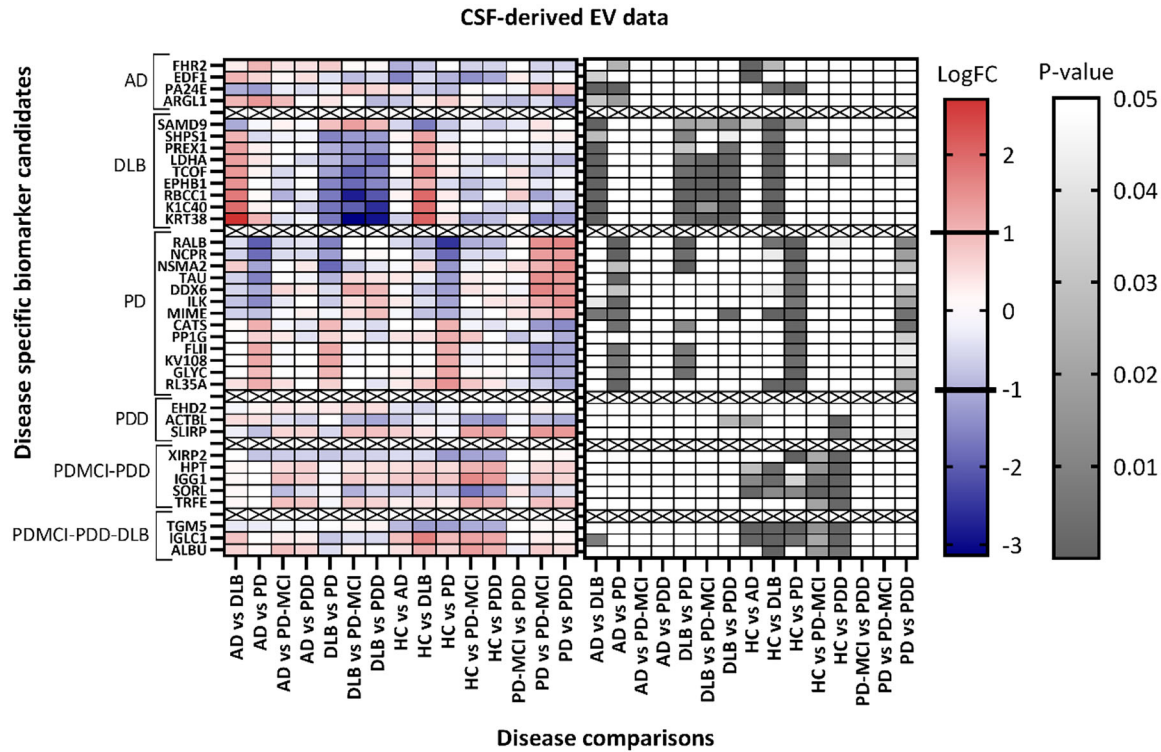


FIGURE 8 Visualisation of the log₂ fold change (LogFC) values and *p*-values for the 37 selected disease specific biomarker candidates, as retrieved by limma differential analysis in the CSF-derived EV data. AD: differentiated HC vs. AD and/or AD vs. DLB, and not amongst non-AD diseases. DLB: differentiated HC vs. DLB and AD vs. DLB, and not amongst non-DLB diseases. PD: differentiated HC vs. PD and PD vs. PDD, and not amongst non-PD diseases. PDD: differentiated HC vs. PDD and AD vs. PDD or DLB vs. PDD, and not amongst non-PD or non-PDD diseases. PDMCI-PDD: differentiated HC vs. PD-MCI and HC vs. PDD. PDMCI-DLB-PDD: differentiated HC vs. the PD continuum and HC vs. DLB. Proteins were considered differentially expressed if the Benjamini–Hochberg-adjusted *p*-value was lower than 0.05 and the absolute LogFC was higher than 1. Exact LogFC and *p*-values for all comparisons can be found in the supplementary Excel, sheet ‘CSF-derived EVs’. AD, Alzheimer’s disease; DLB, dementia with Lewy bodies; HC, healthy controls; PD, Parkinson’s disease; PD-MCI, Parkinson’s disease with mild cognitive impairment; PDD, Parkinson’s disease dementia. Proteins were considered differentially expressed if the Benjamini–Hochberg-adjusted *P*-value was lower than 0.05 and the absolute LogFC was higher than 1.

compare biomarkers between a neurodegenerative disease and healthy controls, but few studies compare neurodegenerative diseases amongst each other. However, plasma NfL has been studied as well, where, for example, Lin et al. (2018) compared the plasma levels of NfL among individuals with MCI, AD, PD and PDD. Their findings indicated higher plasma NfL levels in PDD as compared to PD, with the highest levels observed in AD. The study also established a correlation between high plasma NfL levels and poor cognition in both AD and PD patients, but not with severity of motor symptoms in PD patients (Lin et al., 2018). A study from 2021 reported a correlation between CSF and plasma NfL and that both CSF and plasma NfL levels were correlated with T-Tau (CSF Spearman’s $\rho = 0.36$, *p*-value = 0.024) and $A\beta_{1-42}$ (CSF Spearman’s $\rho = -0.26$, *p*-value <0.001), and confirmed the increase of CSF and plasma NfL in AD compared to HC, but not for DLB (Aamodt et al., 2021). In the SPIN cohort, another study found that CSF NfL levels were higher in males than females, and there was a positive correlation between NfL and both T-Tau and pTau181, and, again, a negative correlation with $A\beta_{1-42}$. The researchers also evidenced a positive correlation between NfL levels and age (Spearman’s $\rho = 0.490$, *p*-value <0.001) (Delaby et al., 2020). In our study, a positive correlation was found of CSF NfL with CSF pTau181, and a negative correlation with CSF $A\beta_{1-42}/A\beta_{1-40}$, reproducing the results from the SPIN cohort. Furthermore, as expected, a correlation between NfL levels and age was detected (Spearman’s $\rho = 0.372$, *p* = 0.0198). Struyfs et al. (2015), using a standard ELISA, also demonstrated a significant decline in CSF $A\beta_{1-42}$, $A\beta_{1-42}/T$ -Tau, $A\beta_{1-42}/p$ Tau181 in AD compared to non-AD, which was replicated in our study. T-Tau and pTau181, in contrast, were elevated in the AD CSF samples in their samples, as expected. These analytes were not significantly different in this study, which can be explained by the small number of samples in this experiment, or it could show that our samples were taken in an early stage of the AD continuum. However, these samples were not provided with an MMSE score. In our study, non-purified CSF samples from DLB/PDD in comparison to those from HC were only found to be downregulated for $A\beta_{1-42}/p$ Tau181 and $A\beta_{1-42}/T$ -Tau. Similarly, the team of Delaby observed decreased levels of $A\beta_{1-42}$ in CSF of DLB patients compared to control subjects (Delaby et al., 2022). Recently, the European DLB consortium has also published results of tau dysregulation in DLB (Di Censo et al., 2020), and Ferreira et al. (2020) discuss $A\beta$ and tau changes in DLB as well. Regarding the comparison of neurodegenerative diseases amongst each other, a study from 2011 (Aerts et al., 2011) compared CSF AD and DLB biomarkers, and while $A\beta_{1-42}$ was not different, T-Tau and

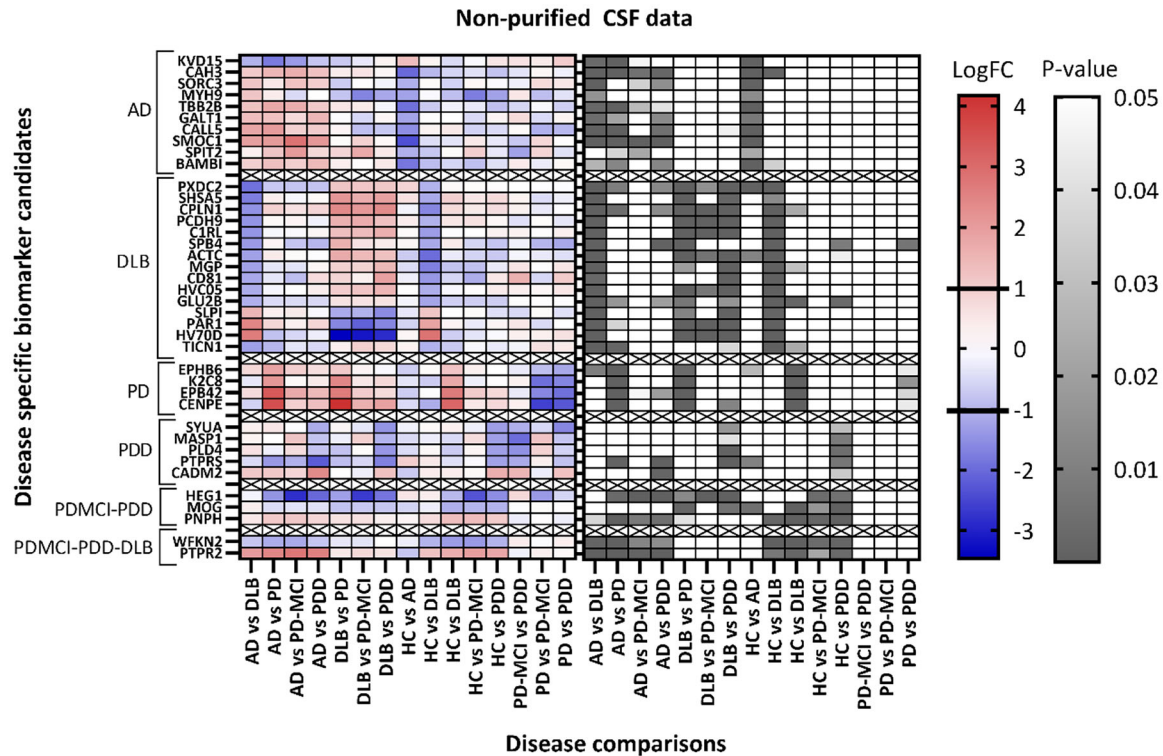


FIGURE 9 Visualisation of the log₂ fold change (LogFC) values and *p*-values for the 39 selected disease specific biomarker candidates, as retrieved by limma differential analysis in the non-purified CSF data. AD: differentiated HC vs. AD and/or AD vs. DLB, and not amongst non-AD diseases. DLB: differentiated HC vs. DLB and AD vs. DLB, and not amongst non-DLB diseases. PD: differentiated HC vs. PD and PD vs. PDD, and not amongst non-PD diseases. PDD: differentiated HC vs. PDD and AD vs. PDD or DLB vs. PDD, and not amongst non-PD or non-PDD diseases. PDMCI-PDD: differentiated HC vs. PD-MCI and HC vs. PDD. PDMCI-DLB-PDD: differentiated HC vs. the PD continuum and HC vs. DLB. Proteins were considered differentially expressed if the Benjamini–Hochberg-adjusted *P*-value was lower than 0.05 and the absolute LogFC was higher than 1. Exact LogFC and *p*-values for all comparisons can be found in the supplementary Excel, sheet ‘non-purified CSF’. AD, Alzheimer’s disease; DLB, dementia with Lewy bodies; HC, healthy controls; PD, Parkinson’s disease; PD-MCI, Parkinson’s disease with mild cognitive impairment; PDD, Parkinson’s disease dementia. Proteins were considered differentially expressed if the Benjamini–Hochberg-adjusted *p*-value was lower than 0.05 and the absolute LogFC was higher than 1.

pTau181 were significantly elevated in AD. In our study, $A\beta_{1-42}$ was shown to be differentially expressed between AD and PDD. This could be explained by the fact that not all PDD and DLB patients exhibit amyloid plaques and NFTs, and thus the results depend on the included patients and their co-pathology. In our study, $A\beta_{1-42}$ was elevated in PDD compared to AD. However, less studies have been performed on PDD and DLB regarding these analytes (Struyfs et al., 2015). For CSF-derived EV samples, none of the Simoa results were shown to be significant. Moreover, some samples were not measured because they were below the LOD. If wanting to reach this LOD, much more volume would be needed of the respective CSF-derived EV samples, which should be taken into account when weighing the advantages over the disadvantages over non-purified CSF. The Simoa data thus initially have failed to show evidence for the hypothesis that EVs might be transmitting the known pathological proteins in the brain this way. Furthermore, it showed the challenges of using EV-enriched samples over non-purified samples in such targeted approach. For the ExoView and Simoa experiments, a limited number of kits were available and samples had to be selected. In these cases, PD-MCI samples were not analysed. For LC-MS/MS, all available samples were included.

Using untargeted proteomics, on the other hand, similar biological information can be acquired but without prior knowledge of clinically relevant proteins. With LC-MS/MS, significant data was extracted from both sample types and differentially expressed proteins were selected. We observed a greater number of differentially expressed proteins in CSF-derived EV samples ($N = 276$) compared to non-purified CSF ($N = 169$), with minimal overlap between both datasets. This finding suggests that CSF-derived EV samples may be more suitable for the discovery phase of a biomarker study, due to the removal of more abundant proteins, resulting in a narrower dynamic range. Data of both sample types, therefore, complement each other. Notably, a larger proportion of the potential biomarkers in CSF-derived EVs, pointed towards neurodegeneration, or in extend to a state of disease in general. For instance, several ribosomal proteins showed altered expression, which in many diseases show up as altered. Two potential markers for neurodegeneration in general were identified in non-purified CSF, while 33 markers were found in CSF-derived EV. As more disease-specific markers, we selected a total of 39 markers as the most promising markers identified in non-purified CSF, and 37 markers across the different included diseases in the CSF-derived EV data. Regarding AD, 10 markers (IGKV3D-15, CA3, SORCS3, MYH9, TUBB2B, GALNT1, CALML5, SMOC1, SPINT2, BAMBI) differentiated AD from the other diseases in

non-purified CSF, and four (CFHR2, EDF1, PLA2G4E, ARGLU1) achieved the same in CSF-derived EVs. For DLB, PD and PDD the numbers were as follows: 15 markers (PLXDC2, SHISA5, CPLANE1, PCDH9, C1RL, SERPINB4, ACTC1, MGP, CD81, IGHV3-30-5, PRKCSH, SLPI, F2R, IGHV2-70D, SPOCK1), 4 markers (EPHB6, KRT8, EPB42, CENPE) and 5 markers (SNCA, MASPI, PLD4, PTPRS, CADM2) in non-purified CSF, and 9 markers (SAMD9, SIRPA, PREX1, LDHA, TCOF1, EPHB1, RBIC1, KRT40, KRT38), 13 markers (RALB, POR, SMPD3, MAPT, DDX6, ILK, OGN, CTSS, PPP1CC, FLII, IGKV1-8, SHMT1, RPL35A), and 3 markers (EHD2, ACTBL2, SLIRP) in CSF-derived EVs, respectively. Considering DLB and PDD as two distinct diseases, 3 markers (HEG1, MOG, PNP) were able to detect PDD in the MCI stage in non-purified CSF, while five markers (XIRP2, HP, IGG1, SORL1, TF) accomplished this in CSF-derived EVs. On the other hand, when regarding DLB and PDD as the same disease, two markers (WFIKKN2, PTPRN2) detected dementia in the MCI stage in non-purified CSF, and three markers (TGM5, IGLC1, ALB) did so in CSF-derived EVs. For non-purified CSF, nine proteins of the total selected proteins also showed up in the network analysis. For CSF-derived EVs, 16 proteins of the network analysis were selected as general neurodegeneration markers, and 11 proteins for DLB or the PD continuum. The selected markers were compared to MarkerDB (Wishart et al., 2021), a database comprising 26,374 genetic biomarkers. Upon matching the selected most-promising non-purified CSF markers with this database, ACTC1 (Alpha cardiac muscle 1 Actin) was identified as a known genetic biomarker for familial hypertrophic cardiomyopathy, MYH9 (Myosin-9) for genetic deafness, and SNCA (α -synuclein) for DLB and PD. From the selected most-promising CSF-derived EV markers, six were found in the database: PPT1 (Palmitoyl-protein thioesterase 1) for neuronal ceroid lipofuscinosis, just as SMPD3 (Sphingomyelin phosphodiesterase), MYO6 (Unconventional myosin-VI) for genetic deafness, MAPT (Microtubule-associated protein tau) for PD and progressive supranuclear palsy, TGM5 (Protein-glutamine gamma-glutamyltransferase 5) for inborn genetic disease, and SORL1 (Sortilin-related receptor) for AD. Of these, ACTC1 is downregulated in DLB compared to AD, PD, PDMCI, PDD and HC; SNCA (SYUA) is downregulated in PDD compared to HC or DLB; MYH9 is downregulated in AD compared to HC or DLB. For CSF-derived EVs, PPT1 and MYO6, as markers for neurodegeneration in general, are downregulated in AD, DLB, PD, PDMCI and PDD compared to HC; SMPD3 is downregulated in PD compared to AD, DLB, HC and PDD; MAPT is downregulated in PD compared to AD, HC and PDD; TGM5 is downregulated in DLB, PD, PDMCI and PDD compared to HC; SORL1 is downregulated in PDMCI and PDD compared to HC. When considering both sample types together, a total of nine potential markers were found in the database, with only one marker also appearing in the MarkerDB protein biomarker section (consisting of 142 entries): TAU for AD (investigational). In our study, MAPT came forward as a biomarker for PD in CSF-derived EVs. Other potential biomarkers have previously been published to distinguish AD from HC. Muraoka et al. (2020) published three promising biomarker candidates to identify the conversion of MCI to AD. Neither of these showed to be differentially significant in our data of non-purified CSF or CSF-derived EVs. However, of those, NPEPPS and PTGFRN were identified in our CSF-derived EVs. Similarly to their third protein of interest, that is, HSPA1A, other heat shock proteins were differentially expressed in our CSF-derived EVs. In our data, HSP90AA4P differentiated HC from PD and HC from PD-MCI, and HSP90AA5P differentiated HC from PD. None of the three proteins were identified in non-purified CSF. In 2023, the study of Chatterjee et al. (2023) showed 26 upregulated proteins in AD, and 88 downregulated proteins. Of the upregulated proteins, four were identified in our non-purified CSF data of which two were differentially expressed among at least two groups (MGP, CFH). Five of their upregulated proteins were identified in our CSF-derived EV data, but none were differentially expressed. In our data, MGP was downregulated in DLB in comparison to AD, PDD and HC. CFH was upregulated in AD versus PD. Of the 88 downregulated proteins, 10 were identified in our non-purified CSF data (of which (6) S100A8, CTSB, TXN, PIP, DSG1, ASAH1 were differentially expressed) and 23 in our CSF-derived EV data (of which (7) S100A6, DSP, S100A11, CFHR2, ATP1A2, ACTBL2, KPRP were differentially expressed). Neither of these seven proteins was dysregulated specifically in AD according to our data. These results show the importance of including clinically similar diseases in a biomarker study, as specificity of such markers is crucial to avoid misdiagnosing. Recently, a paper was published comparing the non-purified CSF proteome of DLB, measured with Olink, with non-purified CSF from healthy controls and from AD patients (Del Campo et al., 2023). Of the differentially expressed proteins in their dataset, seven proteins were differentially expressed in our datasets as well, between at least two of our included groups (AD vs. DLB, AD vs. PD continuum, DLB vs. PD continuum, HC vs. AD, HC vs. DLB and/or HC vs. PD continuum). From these seven proteins, six were identified in non-purified CSF, and three in CSF-derived EVs, with two overlapping in both. Of these, WFIKKN2 passed our potential biomarker selection in non-purified CSF (Table 7, category PDMCI-DLB-PDD). WFIKKN2 is a protease-inhibitor, primarily expressed in ovary, testis and brain. More specifically, according to The Human Protein Atlas, it is highly expressed in the choroid plexus, providing an explanation for its presence in CSF. Notably, according to our knowledge, this protein was previously not linked to dementia.

In order to evaluate biomarkers, sensitivity and specificity analysis, with the help of ROC curves, is commonly carried out. However, this could not be done since in this biomarker discovery study, complex data from mass spectrometry is acquired that is analysed by limma, offering a complex model including empirical Bayes variance adjusting and correcting for co-variates. With a simpler, targeted proteomic approach in the validation study, sensitivity and specificity will be explored for individual markers as well as a combination of markers. It is recommended to explore highly sensitive targeted proteomic techniques for validation in CSF-derived EV samples, as supported by the findings of our Simoa experiments.

To fully investigate the benefits of CSF-EV derived samples compared to non-purified CSF, it is essential to validate all the identified biomarker candidates in both sample types. In particular, validating the markers that demonstrate the ability to

differentiate between AD and DLB/PDD, where current biomarkers have limited performance, can significantly advance the field. Lastly, it is important to consider other, less-invasive biofluids, such as plasma, or more specific, brain-derived EVs from plasma.

We have submitted all relevant data of our experiments to the EV-TRACK knowledgebase (EV-TRACK ID: EV230591) (Van Deun et al., 2017).

5 | CONCLUSION

We were able to successfully perform label-free proteomics not only on non-purified CSF but also on CSF-derived EVs, enriched by SmartSEC HT. We observed a greater number of differentially expressed proteins in CSF-derived EV samples compared to non-purified CSF, with minimal overlap between both datasets. This finding suggests that CSF-derived EV samples may be more helpful in the discovery phase of a biomarker study. Notably, a larger proportion of the potential biomarkers in CSF-derived EVs, pointed towards neurodegeneration, or in extend to a state of disease in general. Although with Simoa, we could not show this for $A\beta$ or Tau, our LC-MS/MS findings suggest that CSF-derived EVs spread disease-altering proteins, albeit not necessarily the most disease-specific ones. As more disease-specific markers, we selected a total of 39 markers as the most promising markers identified in non-purified CSF, and 37 markers across the different included diseases in the CSF-derived EV data. Since of all selected proteins, only nine showed up as known genetic biomarkers, it is necessary to validate all proteins in a larger, independent cohort study. This should be performed on both sample types since further investigations are inquired to determine whether the CSF-derived EV potential biomarkers can also be detected in non-purified CSF using targeted proteomics. This way, a comprehensive understanding of the biomarker's presence and detectability can be obtained. When considering targeted proteomics, non-purified samples may offer a more practical solution as it requires a smaller amount of material compared to EV-enriched samples. Furthermore, it is important to consider other, less-invasive biofluids, such as plasma, or more specific brain-derived EVs from plasma. Nevertheless, in this study, initial key steps were made identifying new leads for future validations.

AUTHOR CONTRIBUTIONS

Yael Hirschberg: Investigation; methodology; writing—original draft. **Natalia Valle-Tamayo:** Investigation; methodology; resources; writing—review and editing. **Oriol Dols-Icardo:** Investigation; supervision; writing—review and editing. **Sebastian Engelborghs:** Resources; writing—review and editing. **Bart Buelens:** Methodology. **Yannick Vermeiren:** Methodology; supervision; writing—review and editing. **Kurt Boonen:** Methodology; supervision; writing—review and editing. **Inge Mertens:** Conceptualization; project administration; supervision; writing—review and editing.

ACKNOWLEDGEMENTS

We express our gratitude to VITO (Flemish Institute for Technological Research, Mol, Belgium) for providing the funding for this study. N. Valle-Tamayo is supported by the Carlos III Health Institute (FI22/00077), O. Dols-Icardo is supported by the Alzheimer's Association (AARF-22-924456). We acknowledge the endeavours of our colleagues from ZNA-Middelheim and Hoge Beuken (P.P. De Deyn, J. Goeman and colleagues) for deep clinical phenotyping of the clinical subjects included, as well as for clinical follow-up of the population included, for 10% of the population even till death. We acknowledge the neuropathologists of the IBB-Neurobiobank (J.J. Martin, A. Sieben) for providing us with the neuropathological data and diagnoses. We are also grateful to the IBB-Neurobiobank for providing us with valuable CSF samples. Additionally, we extend our appreciation to the data science consulting company BioLizard (Ghent, Belgium) for their help in conducting the differential analysis. Furthermore, we would like to acknowledge the Department of Bioscience Engineering at the University of Antwerp (Antwerp, Belgium) for their kind support in granting us access to their microplate reader.

CONFLICT OF INTEREST STATEMENT

SE received unrestricted research grants from ADx Neurosciences and Janssen Pharmaceutica (paid to institution), consulting fees from Eisai, icometrix, Novartis (paid to institution), personal consulting fees from Roche and Biogen, personal honoraria from Eisai, Roche and travel support from Biogen. Patent EP3452830B1 (institution), member of SMB/SAB for EU-H2020 project RECAE and member of the DSMB of PRImus-AD. VP of Belgian Dementia Council (unpaid). The other authors declare no conflict of interest.

ORCID

Yael Hirschberg  <https://orcid.org/0000-0001-7810-9303>

Roosmarijn E. Vandenbroucke  <https://orcid.org/0000-0002-8327-620X>

REFERENCES

- Aamodt, W. W., Waligorska, T., Shen, J., Tropea, T. F., Siderowf, A., Weintraub, D., Grossman, M., Irwin, D., Wolk, D. A., Xie, S. X., Trojanowski, J. Q., Shaw, L. M., & Chen-Plotkin, A. S. (2021). Neurofilament light chain as a biomarker for cognitive decline in Parkinson disease. *Movement Disorders*, *36*, 2945–2950.
- Aarsland, D., Bronnick, K., Ehrt, U., De Deyn, P. P., Tekin, S., Emre, M., & Cummings, J. L. (2007). Neuropsychiatric symptoms in patients with Parkinson's disease and dementia: Frequency, profile and associated care giver stress. *Journal of Neurology, Neurosurgery, and Psychiatry*, *78*, 36–42.
- Aerts, M. B., Esselink, R. A., Claassen, J. A., Abdo, W. F., Bloem, B. R., & Verbeek, M. M. (2011). CSF tau, Abeta42, and MHPG differentiate dementia with Lewy bodies from Alzheimer's disease. *Journal of Alzheimer's Disease*, *27*, 377–384.
- American Psychiatric Association. (2010). *DSM-IV-TR: Diagnostic and statistical manual of mental disorders*. American Psychiatric Association.
- Asgari, M., De Zelicourt, D. A., & Kurtcuoglu, V. (2017). Barrier dysfunction or drainage reduction: Differentiating causes of CSF protein increase. *Fluids Barriers CNS*, *14*, 14.
- Bachurski, D., Schuldner, M., Nguyen, P. H., Malz, A., Reiners, K. S., Grenzi, P. C., Babatz, F., Schauss, A. C., Hansen, H. P., Hallek, M., & Pogge Von Strandmann, E. (2019). Extracellular vesicle measurements with nanoparticle tracking analysis—An accuracy and repeatability comparison between NanoSight NS300 and ZetaView. *Journal of Extracellular Vesicles*, *8*, 1596016.
- Ballard, C., & Howard, R. (2006). Neuroleptic drugs in dementia: Benefits and harm. *Nature Reviews Neuroscience*, *7*, 492–500.
- Bousiges, O., & Blanc, F. (2022). Biomarkers of dementia with Lewy bodies: Differential diagnostic with Alzheimer's Disease. *International Journal of Molecular Sciences*, *23*(12), 6371.
- Burger, B., Vaudel, M., & Barsnes, H. (2021). Importance of block randomization when designing proteomics experiments. *Journal of Proteome Research*, *20*, 122–128.
- Chatterjee, M., Ozdemir, S., Kunadt, M., Koel-Simmellink, M., Boiten, W., Piepkorn, L., Pham, T. V., Chiasserini, D., Piersma, S. R., Knol, J. C., Mobius, W., Mollenhauer, B., Van Der Flier, W. M., Jimenez, C. R., Teunissen, C. E., Jahn, O., & Schneider, A. (2023). Clq is increased in cerebrospinal fluid-derived extracellular vesicles in Alzheimer's disease: A multi-cohort proteomics and immuno-assay validation study. *Alzheimer's & Dementia*, *19*(11), 4828–4840.
- Comfort, N., Bloomquist, T. R., Shephard, A. P., Petty, C. R., Cunningham, A., Hauptman, M., Phipatanakul, W., & Baccarelli, A. (2021). Isolation and characterization of extracellular vesicles in saliva of children with asthma. *Extracellular Vesicles and Circulating Nucleic Acids*, *2*, 29–48.
- Cox, J., & Mann, M. (2008). MaxQuant enables high peptide identification rates, individualized p.p.b.-range mass accuracies and proteome-wide protein quantification. *Nature Biotechnology*, *26*, 1367–1372.
- Delaby, C., Alcolea, D., Carmona-Iragui, M., Illan-Gala, I., Morenas-Rodriguez, E., Barroeta, I., Altuna, M., Estelles, T., Santos-Santos, M., Turon-Sans, J., Munoz, L., Ribosa-Nogue, R., Sala-Matavera, I., Sanchez-Saudinos, B., Subirana, A., Videla, L., Benejam, B., Sirisi, S., Lehmann, S., ... Lleo, A. (2020). Differential levels of Neurofilament Light protein in cerebrospinal fluid in patients with a wide range of neurodegenerative disorders. *Scientific Reports*, *10*, 9161.
- Delaby, C., Estelles, T., Zhu, N., Arranz, J., Barroeta, I., Carmona-Iragui, M., Illan-Gala, I., Santos-Santos, M. A., Altuna, M., Sala, I., Sanchez-Saudinos, M. B., Videla, L., Valldeu, S., Subirana, A., Tondo, M., Blanco-Vaca, F., Lehmann, S., Belbin, O., Blesa, R., ... Alcolea, D. (2022). The Abeta1-42/Abeta1-40 ratio in CSF is more strongly associated to tau markers and clinical progression than Abeta1-42 alone. *Alzheimer's Research & Therapy*, *14*, 20.
- Del Campo, M., Vermunt, L., Peeters, C. F. W., Sieben, A., Hok, A. H. Y. S., Lleo, A., Alcolea, D., van Nee, M., Engelborghs, S., Van Alphen, J. L., Arezoumandan, S., Chen-Plotkin, A., Irwin, D. J., Van Der Flier, W. M., Lemstra, A. W., & Teunissen, C. E. (2023). CSF proteome profiling reveals biomarkers to discriminate dementia with Lewy bodies from Alzheimer's disease. *Nature Communications*, *14*, 5635.
- Deng, F., Ratri, A., Deighan, C., Daaboul, G., Geiger, P. C., & Christenson, L. K. (2022). Single-particle interferometric reflectance imaging characterization of individual extracellular vesicles and population dynamics. *Journal of visualized experiments: JoVE*, *179*, <https://doi.org/10.3791/62988>
- Devanand, D. P., Lee, S., Huey, E. D., & Goldberg, T. E. (2022). Associations between neuropsychiatric symptoms and neuropathological diagnoses of Alzheimer disease and related dementias. *JAMA Psychiatry*, *79*, 359–367.
- Di Censo, R., Abdelnour, C., Blanc, F., Bousiges, O., Lemstra, A. W., van Steenoven, I., Onofri, M., Aarsland, D., & Bonanni, L., European DLB consortium. (2020). CSF tau proteins correlate with an atypical clinical presentation in dementia with Lewy bodies. *Journal of Neurology, Neurosurgery, and Psychiatry*, *91*, 109–110.
- Dubois, B., Feldman, H. H., Jacova, C., Hampel, H., Molinuevo, J. L., Blennow, K., Dekosky, S. T., Gauthier, S., Selkoe, D., Bateman, R., Cappa, S., Crutch, S., Engelborghs, S., Frisoni, G. B., Fox, N. C., Galasko, D., Habert, M. O., Jicha, G. A., Nordberg, A., ... Cummings, J. L. (2014). Advancing research diagnostic criteria for Alzheimer's disease: The IWG-2 criteria. *Lancet Neurology*, *13*, 614–629.
- Dujardin, S., Begard, S., Cailliez, R., Lachaud, C., Delattre, L., Carrier, S., Loyens, A., Galas, M. C., Bousset, L., Melki, R., Auregan, G., Hantraye, P., Brouillet, E., Buee, L., & Colin, M. (2014). Ectosomes: A new mechanism for non-exosomal secretion of tau protein. *PLoS ONE*, *9*, e100760.
- Engelborghs, S., De Vreese, K., Van De Castele, T., Vanderstichele, H., Van Everbroeck, B., Cras, P., Martin, J. J., Vanmechelen, E., & De Deyn, P. P. (2008). Diagnostic performance of a CSF-biomarker panel in autopsy-confirmed dementia. *Neurobiology of Aging*, *29*, 1143–1159.
- Engelborghs, S., Marescau, B., & De Deyn, P. P. (2003). Amino acids and biogenic amines in cerebrospinal fluid of patients with Parkinson's disease. *Neurochemical Research*, *28*, 1145–1150.
- Ferman, T. J., Boeve, B. F., Smith, G. E., Lin, S. C., Silber, M. H., Pedraza, O., Wszolek, Z., Graff-Radford, N. R., Uitti, R., Van Gerpen, J., Pao, W., Knopman, D., Pankratz, V. S., Kantarci, K., Boot, B., Parisi, J. E., Dugger, B. N., Fujishiro, H., Petersen, R. C., & Dickson, D. W. (2011). Inclusion of RBD improves the diagnostic classification of dementia with Lewy bodies. *Neurology*, *77*, 875–882.
- Ferreira, D., Przybelski, S. A., Lesnick, T. G., Lemstra, A. W., Londos, E., Blanc, F., Nedelska, Z., Schwarz, C. G., Graff-Radford, J., Senjem, M. L., Fields, J. A., Knopman, D. S., Savica, R., Ferman, T. J., Graff-Radford, N. R., Lowe, V. J., Jack, Jr., C. R., Petersen, R. C., Mollenhauer, B., ... Kantarci, K. (2020). β -Amyloid and tau biomarkers and clinical phenotype in dementia with Lewy bodies. *Neurology*, *95*, e3257–e3268.
- Fiandaca, M. S., Kapogiannis, D., Mapstone, M., Boxer, A., Eitan, E., Schwartz, J. B., Abner, E. L., Petersen, R. C., Federoff, H. J., Miller, B. L., & Goetzl, E. J. (2015). Identification of preclinical Alzheimer's disease by a profile of pathogenic proteins in neurally derived blood exosomes: A case-control study. *Alzheimer's & Dementia*, *11*, 600–607. e1.
- Fritz, N. E., Kegelmeyer, D. A., Kloos, A. D., Linder, S., Park, A., Katakai, M., Adeli, A., Agrawal, P., Scharre, D. W., & Kostyk, S. K. (2016). Motor performance differentiates individuals with Lewy body dementia, Parkinson's and Alzheimer's disease. *Gait & Posture*, *50*, 1–7.
- Hansson, O., Janelidze, S., Hall, S., Magdalinou, N., Lees, A. J., Andreasson, U., Norgren, N., Linder, J., Forsgren, L., Constantinescu, R., Zetterberg, H., & Blennow, K., Swedish BioFINDER study. (2017). Blood-based NfL: A biomarker for differential diagnosis of Parkinsonian disorder. *Neurology*, *88*, 930–937.
- Hirschberg, Y., Boonen, K., Schildermans, K., Van Dam, A., Pintelon, I., Vandendriessche, C., Velimirovic, M., Jacobs, A., Vandenbroucke, R. E., Nelissen, I., Vermeiren, Y., & Mertens, I. (2022). Characterising extracellular vesicles from individual low volume cerebrospinal fluid samples, isolated by SmartSEC. *Journal of Extracellular Biology*, *1*(9), e55.

- Jellinger, K. A., & Korczyn, A. D. (2018). Are dementia with Lewy bodies and Parkinson's disease dementia the same disease? *BMC Medicine [Electronic Resource]*, 16, 34.
- Kanmert, D., Cantlon, A., Muratore, C. R., Jin, M., O'malley, T. T., Lee, G., Young-Pearse, T. L., Selkoe, D. J., & Walsh, D. M. (2015). C-terminally truncated forms of tau, but not full-length tau or its C-terminal fragments, are released from neurons independently of cell death. *Journal of Neuroscience*, 35, 10851–10865.
- Li, T. R., Yao, Y. X., Jiang, X. Y., Dong, Q. Y., Yu, X. F., Wang, T., Cai, Y. N., & Han, Y. (2022). β -amyloid in blood neuronal-derived extracellular vesicles is elevated in cognitively normal adults at risk of Alzheimer's disease and predicts cerebral amyloidosis. *Alzheimer's Research & Therapy*, 14, 66.
- Lin, Y. S., Lee, W. J., Wang, S. J., & Fuh, J. L. (2018). Levels of plasma neurofilament light chain and cognitive function in patients with Alzheimer or Parkinson disease. *Scientific Reports*, 8, 17368.
- Mattsson, N., Cullen, N. C., Andreasson, U., Zetterberg, H., & Blennow, K. (2019). Association between longitudinal plasma neurofilament light and neurodegeneration in patients with Alzheimer disease. *JAMA Neurology*, 76, 791–799.
- Mckeith, I. G., Boeve, B. F., Dickson, D. W., Halliday, G., Taylor, J. P., Weintraub, D., Aarsland, D., Galvin, J., Attems, J., Ballard, C. G., Bayston, A., Beach, T. G., Blanc, F., Bohnen, N., Bonanni, L., Bras, J., Brundin, P., Burn, D., Chen-Plotkin, A., ... Kosaka, K. (2017). Diagnosis and management of dementia with Lewy bodies: Fourth consensus report of the DLB Consortium. *Neurology*, 89, 88–100.
- McKeith, I. G., Dickson, D. W., Lowe, J., Emre, M., O'Brien, J. T., Feldman, H., Cummings, J., Duda, J. E., Lippa, C., Perry, E. K., Aarsland, D., Arai, H., Ballard, C. G., Boeve, B., Burn, D. J., Costa, D., Del Ser, T., & Dubois, B., Consortium on DLB. (2005). Diagnosis and management of dementia with Lewy bodies: Third report of the DLB Consortium. *Neurology*, 65, 1863–1872.
- Mckeith, I. G., Galasko, D., Kosaka, K., Perry, E. K., Dickson, D. W., Hansen, L. A., Salmon, D. P., Lowe, J., Mirra, S. S., Byrne, E. J., Lennox, G., Quinn, N. P., Edwardson, J. A., Ince, P. G., Bergeron, C., Burns, A., Miller, B. L., Lovestone, S., Collerton, D., ... Perry, R. H. (1996). Consensus guidelines for the clinical and pathologic diagnosis of dementia with Lewy bodies (DLB): Report of the consortium on DLB international workshop. *Neurology*, 47, 1113–1124.
- Mckhann, G., Drachman, D., Folstein, M., Katzman, R., Price, D., & Stadlan, E. M. (1984). Clinical diagnosis of Alzheimer's disease: Report of the NINCDS-ADRDA Work Group under the auspices of Department of Health and Human Services Task Force on Alzheimer's Disease. *Neurology*, 34, 939–944.
- Mckhann, G. M., Knopman, D. S., Chertkow, H., Hyman, B. T., Jack, C. R., Kawas Jr, C. H., Klunk, W. E., Koroshetz, W. J., Manly, J. J., Mayeux, R., Mohs, R. C., Morris, J. C., Rossor, M. N., Scheltens, P., Carrillo, M. C., Thies, B., Weintraub, S., & Phelps, C. H. (2011). The diagnosis of dementia due to Alzheimer's disease: Recommendations from the National Institute on Aging-Alzheimer's Association workgroups on diagnostic guidelines for Alzheimer's disease. *Alzheimer's & Dementia*, 7, 263–269.
- Meier, F., Brunner, A. D., Koch, S., Koch, H., Lubeck, M., Krause, M., Goedecke, N., Decker, J., Kosinski, T., Park, M. A., Bache, N., Hoerning, O., Cox, J., Rather, O., & Mann, M. (2018). Online Parallel Accumulation-Serial Fragmentation (PASEF) with a novel trapped ion mobility mass spectrometer. *Molecular & Cellular Proteomics*, 17, 2534–2545.
- Muraoka, S., Jedrychowski, M. P., Yamamandra, K., Ikezu, S., Gygi, S. P., & Ikezu, T. (2020). Proteomic profiling of extracellular vesicles derived from cerebrospinal fluid of Alzheimer's disease patients: A pilot study. *Cells*, 9(9), 1959.
- Outeiro, T. F., Koss, D. J., Erskine, D., Walker, L., Kurzawa-Akanbi, M., Burn, D., Donaghy, P., Morris, C., Taylor, J. P., Thomas, A., Attems, J., & Mckeith, I. (2019). Dementia with Lewy bodies: An update and outlook. *Molecular Neurodegeneration*, 14, 5.
- Phipson, B., Lee, S., Majewski, I. J., Alexander, W. S., & Smyth, G. K. (2016). Robust hyperparameter estimation protects against hypervariable genes and improves power to detect differential expression. *The Annals of Applied Statistics*, 10, 946–963.
- Prince, M., Ali, G. C., Guerchet, M., Prina, A. M., Albanese, E., & Wu, Y. T. (2016). Recent global trends in the prevalence and incidence of dementia, and survival with dementia. *Alzheimer's Research & Therapy*, 8, 23.
- Seyfert, S., Kunzmann, V., Schwertfeger, N., Koch, H. C., & Faulstich, A. (2002). Determinants of lumbar CSF protein concentration. *Journal of Neurology*, 249, 1021–1026.
- Slaets, S., Le Bastard, N., Theuns, J., Sleegers, K., Verstraeten, A., De Leenheir, E., Luyckx, J., Martin, J. J., Van Broeckhoven, C., & Engelborghs, S. (2013). Amyloid pathology influences abeta42 cerebrospinal fluid levels in dementia with lewy bodies. *Journal of Alzheimer's Disease*, 35, 137–146.
- Smirnov, D. S., Galasko, D., Edland, S. D., Filoteo, J. V., Hansen, L. A., & Salmon, D. P. (2020). Cognitive decline profiles differ in Parkinson disease dementia and dementia with Lewy bodies. *Neurology*, 94, e2076–e2087.
- Somers, C., Struyfs, H., Goossens, J., Niemantsverdriet, E., Luyckx, J., De Roeck, N., De Roeck, E., De Vil, B., Cras, P., Martin, J. J., De Deyn, P. P., Bjerke, M., & Engelborghs, S. (2016). A decade of cerebrospinal fluid biomarkers for Alzheimer's disease in Belgium. *Journal of Alzheimer's Disease*, 54, 383–395.
- Struyfs, H., Niemantsverdriet, E., Goossens, J., Franssen, E., Martin, J. J., De Deyn, P. P., & Engelborghs, S. (2015). Cerebrospinal fluid P-Tau181P: Biomarker for improved differential dementia diagnosis. *Frontiers in Neurology*, 6, 138.
- Stuendl, A., Kunadt, M., Kruse, N., Bartels, C., Moebius, W., Danzer, K. M., Mollenhauer, B., & Schneider, A. (2016). Induction of alpha-synuclein aggregate formation by CSF exosomes from patients with Parkinson's disease and dementia with Lewy bodies. *Brain*, 139, 481–494.
- Szklarczyk, D., Kirsch, R., Koutrouli, M., Nastou, K., Mehryary, F., Hachilif, R., Gable, A. L., Fang, T., Doncheva, N. T., Pyysalo, S., Bork, P., Jensen, L. J., & Von Mering, C. (2023). The STRING database in 2023: Protein-protein association networks and functional enrichment analyses for any sequenced genome of interest. *Nucleic Acids Research*, 51, D638–D646.
- Uemura, N., Uemura, M. T., Luk, K. C., Lee, V. M., & Trojanowski, J. Q. (2020). Cell-to-cell transmission of Tau and alpha-synuclein. *Trends in Molecular Medicine*, 26, 936–952.
- Van Deun, J., Mestdagh, P., Agostinis, P., Akay, Ö., Anand, S., Anckaert, J., Martinez, Z. A., Baetens, T., Beghein, E., Bertier, L., Berx, G., Boere, J., Boukouris, S., Bremer, M., Buschmann, D., Byrd, J. B., Casert, C., & Hendrix, A., EV-TRACK Consortium. (2017). EV-TRACK: Transparent reporting and centralizing knowledge in extracellular vesicle research. *Nature Methods*, 14, 228–232.
- Van Dyck, C. H., Swanson, C. J., Aisen, P., Bateman, R. J., Chen, C., Gee, M., Kanekiyo, M., Li, D., Reyderman, L., Cohen, S., Froelich, L., Katayama, S., Sabbagh, M., Vellas, B., Watson, D., Dhadda, S., Irizarry, M., Kramer, L. D., & Iwatsubo, T. (2023). Lecanemab in early Alzheimer's disease. *New England Journal of Medicine*, 388, 9–21.
- Vann Jones, S. A., & O'Brien, J. T. (2014). The prevalence and incidence of dementia with Lewy bodies: A systematic review of population and clinical studies. *Psychological Medicine*, 44, 673–683.
- Vermeiren, Y., Van Dam, D., Aerts, T., Engelborghs, S., Martin, J. J., & De Deyn, P. P. (2015). The monoaminergic footprint of depression and psychosis in dementia with Lewy bodies compared to Alzheimer's disease. *Alzheimer's Research & Therapy*, 7, 7.
- Wang, Y., Balaji, V., Kaniyappan, S., Kruger, L., Irsen, S., Tepper, K., Chandupatla, R., Maetzler, W., Schneider, A., Mandelkow, E., & Mandelkow, E. M. (2017). The release and trans-synaptic transmission of Tau via exosomes. *Molecular Neurodegeneration*, 12, 5.
- Williams-Gray, C. H., Mason, S. L., Evans, J. R., Foltynie, T., Brayne, C., Robbins, T. W., & Barker, R. A. (2013). The CamPaIGN study of Parkinson's disease: 10-year outlook in an incident population-based cohort. *Journal of Neurology, Neurosurgery, and Psychiatry*, 84, 1258–1264.

- Winston, C. N., Goetzl, E. J., Akers, J. C., Carter, B. S., Rockenstein, E. M., Galasko, D., Masliah, E., & Rissman, R. A. (2016). Prediction of conversion from mild cognitive impairment to dementia with neuronally derived blood exosome protein profile. *Alzheimer's and Dementia (Amsterdam)*, 3, 63–72.
- Wishart, D. S., Bartok, B., Oler, E., Liang, K. Y. H., Budinski, Z., Berjanskii, M., Guo, A., Cao, X., & Wilson, M. (2021). MarkerDB: An online database of molecular biomarkers. *Nucleic Acids Research*, 49, D1259–D1267.
- Wuschek, A., Grahl, S., Pongratz, V., Korn, T., Kirschke, J., Zimmer, C., Hemmer, B., & Muhlau, M. (2019). CSF protein concentration shows no correlation with brain volume measures. *Frontiers in Neurology*, 10, 463.
- Yamada, M., Komatsu, J., Nakamura, K., Sakai, K., Samuraki-Yokohama, M., Nakajima, K., & Yoshita, M. (2020). Diagnostic criteria for dementia with lewy bodies: Updates and future directions. *Journal of Movement Disorders*, 13, 1–10.
- Yoshihara, T., Zaitsu, M., Ito, K., Hanada, R., Chung, E., Yazawa, R., Sakata, Y., Furusho, K., Tsukikawa, H., Chiyoda, T., Matsuki, S., & Irie, S. (2021). Cerebrospinal fluid protein concentration in healthy older Japanese volunteers. *International Journal of Environmental Research and Public Health*, 18(16), 8683.
- Yuyama, K., Sun, H., Sakai, S., Mitsutake, S., Okada, M., Tahara, H., Furukawa, J., Fujitani, N., Shinohara, Y., & Igarashi, Y. (2014). Decreased amyloid-beta pathologies by intracerebral loading of glycosphingolipid-enriched exosomes in Alzheimer model mice. *Journal of Biological Chemistry*, 289, 24488–24498.
- Zolg, D. P., Wilhelm, M., Yu, P., Knaute, T., Zerweck, J., Wenschuh, H., Reimer, U., Schnatbaum, K., & Kuster, B. (2017). PROCAL: A set of 40 peptide standards for retention time indexing, column performance monitoring, and collision energy calibration. *Proteomics*, 17(21), <https://doi.org/10.1002/pmic.201700263>

SUPPORTING INFORMATION

Additional supporting information can be found online in the Supporting Information section at the end of this article.

How to cite this article: Hirschberg, Y., Valle-Tamayo, N., Dols-Icardo, O., Engelborghs, S., Buelens, B., Vandenbroucke, R. E., Vermeiren, Y., Boonen, K., & Mertens, I. (2023). Proteomic comparison between non-purified cerebrospinal fluid and cerebrospinal fluid-derived extracellular vesicles from patients with Alzheimer's, Parkinson's and Lewy body dementia. *Journal of Extracellular Vesicles*, 12, e12383. <https://doi.org/10.1002/jev2.12383>